⌘ *Author's Choice*

THE JOURNAL OF BIOLOGICAL CHEMISTRY VOL. 286, NO. 11, pp. 9079–9096, March 18, 2011

Small Molecule AKAP-Protein Kinase A (PKA) Interaction Disruptors That Activate PKA Interfere with Compartmentalized cAMP Signaling in Cardiac Myocytes*[S]

Received for publication, July 1, 2010, and in revised form, December 12, 2010 Published, JBC Papers in Press, December 22, 2010, DOI 10.1074/jbc.M110.160614

Frank Christian,[a1] Márta Szaszák,[a1] Sabine Friedl,[a] Stephan Drewianka,[b] Dorothea Lorenz,[a] Andrey Goncalves,[a,c] Jens Furkert,[a] Carolyn Vargas,[a] Peter Schmieder,[a] Frank Götz,[a,c] Kerstin Zühlke,[a,c] Marie Moutty,[a,c] Hendrikje Göttert,[a] Mangesh Joshi,[a] Bernd Reif,[a] Hannelore Haase,[c] Ingo Morano,[c] Solveig Grossmann,[a] Anna Klukovits,[d] Judit Verli,[d] Róbert Gáspár,[d] Claudia Noack,[c] Martin Bergmann,[c] Robert Kass,[e] Kornelia Hampel,[b] Dmitry Kashin,[f] Hans-Gottfried Genieser,[f] Friedrich W. Herberg,[g] Debbie Willoughby,[h] Dermot M. F. Cooper,[h] George S. Baillie,[i] Miles D. Houslay,[i] Jens Peter von Kries,[a] Bastian Zimmermann,[b] Walter Rosenthal,[c,j] and Enno Klussmann[a,c2]

From the [a]Leibniz Institute for Molecular Pharmacology, Robert-Rössle-Strasse 10, 13125 Berlin, Germany, [b]Biaffin GmbH & Co. KG, AVZ 2, Heinrich-Plett-Strasse 40, 34132 Kassel, Germany, [c]Max Delbrück Center for Molecular Medicine, Robert-Rössle-Strasse 10, 13125 Berlin, Germany, the [d]Department of Pharmacodynamics and Biopharmacy, University of Szeged, H-6720 Szeged, Eötvös u. 6., Hungary, [e]Columbia University Medical Center, New York, New York 10032, [f]Biolog Life Science Institute, Flughafendamm 9A, 28199 Bremen, Germany, the [g]Department of Biochemistry, University of Kassel, Heinrich-Plett-Strasse 40, 34109 Kassel, Germany, the [h]Department of Pharmacology, University of Cambridge, Tennis Court Road, Cambridge CB2 1 PD, United Kingdom, [i]Neuroscience and Molecular Pharmacology, Wolfson Link and Davidson Buildings, University of Glasgow, University Avenue, Glasgow G12 8QQ, United Kingdom, and [j]Molecular Pharmacology and Cell Biology, Charité-University Medicine Berlin, Thielallee 73, 14195 Berlin, Germany

A-kinase anchoring proteins (AKAPs) tether protein kinase A (PKA) and other signaling proteins to defined intracellular sites, thereby establishing compartmentalized cAMP signaling. AKAP-PKA interactions play key roles in various cellular processes, including the regulation of cardiac myocyte contractility. We discovered small molecules, 3,3′-diamino-4,4′-dihydroxydiphenylmethane (FMP-API-1) and its derivatives, which inhibit AKAP-PKA interactions *in vitro* and in cultured cardiac myocytes. The molecules bind to an allosteric site of regulatory subunits of PKA identifying a hitherto unrecognized region that controls AKAP-PKA interactions. FMP-API-1 also activates PKA. The net effect of FMP-API-1 is a selective interference with compartmentalized cAMP signaling. In cardiac myocytes, FMP-API-1 reveals a novel mechanism involved in terminating β-adrenoreceptor-induced cAMP synthesis. In addition, FMP-API-1 leads to an increase in contractility of cultured rat cardiac myocytes and intact hearts. Thus, FMP-API-1 represents not only a novel means to study compartmentalized cAMP/PKA signaling but, due to its effects on cardiac myocytes and intact hearts, provides the basis for a new concept in the treatment of chronic heart failure.

Cyclic AMP (cAMP)-dependent protein kinase (protein kinase A; PKA)[3] is a ubiquitous serine/threonine kinase controlling a variety of cellular functions. PKA holoenzyme consists of a dimer of regulatory subunits (RIα, RIβ, RIIα, or RIIβ) and two catalytic subunits (Cα, Cβ, or Cγ), each bound to an R subunit. RI-containing holoenzyme is termed PKA type I, whereas RII-containing PKA is termed PKA type II. Binding of cAMP to the R subunits induces a conformational change, causing the release and thus activation of the catalytic subunits, which then phosphorylate various substrates (1). Specificity of PKA action is achieved by controlling its cellular localization through a family of A-kinase anchoring proteins (AKAPs).

AKAPs bind PKA through an amphipathic α-helical structure consisting of 14–18 amino acids (RII-binding domain), which interacts with the hydrophobic groove formed by the N-terminal dimerization and docking (D/D) domain of regulatory subunit dimers (2–5). Besides PKA, AKAPs can directly bind various signaling proteins, such as other protein kinases, protein phosphatases, cAMP phosphodiesterases (PDEs), GTP-binding proteins, adaptor proteins, and substrate proteins of PKA. Thus, AKAPs coordinate multiprotein signaling complexes, thereby establishing compartmentalized signaling (6–9).

The functional roles of AKAP-PKA interactions have often been uncovered in *in vitro* and in cell-based studies by disrup-

* This work was supported by Deutsche Forschungsgemeinschaft Forschergruppe 806 Projects KL1415/4-1 and/4-2, European Union Project thera cAMP-proposals 037189, GoBio program of the German Ministry of Education and Science Grants FKZ 0315097 and 0315516, Medical Research Council UK Grant G0600765, Fondation Leducq Grant 06CVD02, and Wellcome Trust Grant RG31760.

[S] The on-line version of this article (available at http://www.jbc.org) contains supplemental Figs. 1–3.

⌘ *Author's Choice*—Final version full access.

[1] These authors contributed equally to this work.

[2] To whom correspondence should be addressed: Anchored Signaling, Max-Delbrück-Centrum für Molekulare Medizin (MDC) Berlin-Buch, Robert-Rössle-Str. 10, 13125 Berlin, Germany. Tel.: 49-30-9406-2596; Fax: 49-30-9497-008. E-mail: enno.klussmann@mdc-berlin.de.

[3] The abbreviations used are: PKA, protein kinase A; AKAP, A-kinase anchoring protein; RII, type II regulatory subunit of PKA; STD, saturation transfer difference; FMP-API-1, 3,3′-diamino-4,4′-dihydroxydiphenylmethane; D/D, dimerization and docking; PDE, phosphodiesterase; SPR, surface plasmon resonance; CNGC, cyclic nucleotide-gated channel(s); 8-AHA-cAMP, 8-(6-aminohexylamino)adenosine-3′,5′-cyclic monophosphate; ISO, isoproterenol; PLN, phospholamban; c-TnI, cardiac troponin I; PGE, prostaglandin E; EP, eicosanoid E prostaglandin receptor.

tion of the interactions using peptides derived from the RII-binding domains of AKAPs. Several such peptides have been developed (6). For example, peptide Ht31 was derived from the RII-binding domain of AKAP-Lbc (10), AKAP *in silico* ($AKAP_{IS}$) was derived from a bioinformatics approach (11), super$AKAP_{IS}$ was derived from $AKAP_{IS}$ (4), and others were derived from the RII-binding domain of AKAP18δ (12). Peptides like these have, for instance, been used to uncouple PKA from AKAPs in cardiac myocytes and thereby to demonstrate that AKAP-PKA interactions facilitate β-adrenoreceptor-induced increases in cardiac myocyte contractility (13).

Although peptides have proven invaluable for such purposes, their restricted membrane permeability and poor oral availability limit their use for therapeutic purposes and in animal studies. These drawbacks may be overcome with small molecules. Various examples show that disruption of protein-protein interactions with small molecules is feasible. Both small molecules interfering with interactions by association with the interacting surfaces or by allosteric binding have been identified (14–16). The specificity and diversity of protein-protein interactions permits highly selective pharmacological interference. Thus, targeting protein-protein interactions with small molecules opens new avenues for the study of molecular mechanisms. In addition, the development of small molecules targeting disease-relevant protein-protein interactions may lead to novel therapeutic strategies, which, potentially, result in higher specificity and fewer side effects.

Here we report the discovery of small molecules that have a dual effect. FMP-API-1 and its derivatives inhibit AKAP-PKA associations and also activate PKA. Using cardiac myocytes, we show that these molecules provide a new means to analyze functions of compartmentalized cAMP/PKA signaling. Moreover, we show that the approach of targeting scaffolding proteins with small molecules may pave the way to a novel concept for the treatment of chronic heart failure.

EXPERIMENTAL PROCEDURES

Generation of Recombinant RII Subunits and AKAP18δ—Recombinant AKAP18δ was generated as a fusion with glutathione *S*-transferase (GST) as described (17). Full-length PKA RIIα (17) was subcloned from pGEX-4T-3 into the Profinity eXact pPAL7 vector, creating a Profinity exact fusion tag N-terminal to the recombinant protein (Bio-Rad). Deletion mutants were amplified by PCR from the RIIα full-length template and cloned into pPAL7 via BamHI and NotI restriction sites. RIIα variants were expressed in *Escherichia coli* (strain Rosetta DE3). Tag-free RIIα proteins were affinity-purified as recommended by the supplier of the Profinity exact fusion tag system (Bio-Rad). The final polishing step was a gel filtration with Superdex 75 (GE Healthcare) in 20 mM HEPES, 300 mM NaCl, pH 7.

ELISA-based Screening of a Small Molecule Library—An ELISA-based assay, established for the detection of the AKAP18δ-RIIα interaction (12), was used for screening a small molecule library (FMP_20.000) with 20,064 compounds in 384-well plates.

Synthesis of FMP-API-1 Analogues—Syntheses of FMP-API-1 and derivatives (Table 1) followed published procedures from commercially available precursors in one or two steps. Purity of all compounds was monitored by reversed-phase HPLC applying a gradient from water to 100% acetonitrile within 60 min at a flow rate of 1 ml/min. Exemplary procedures are briefly described below.

Synthesis of FMP-API-1—Bis-(4-hydroxyphenylmethane) was nitrated by diluted nitric acid to yield 3,3′-dinitro-4,4′-dihydroxydiphenylmethane, which was subsequently reduced with palladium/charcoal (10%) in a hydrogen atmosphere. Flash chromatography on silica with dichloromethane/methanol (15:1) gave pure 3,3′-diamino-4,4′-dihydroxydiphenylmethane as a gray solid. $C_{13}H_{14}N_2O_2$; MW 230,3; CAS [16523-28-7]; purity 99.4%; yield 70%; UV: λ_{max} = 293 nm.

Synthesis of 4-Benzyl-pyrocatechol (Compound FMP-API-1/27)—Compound FMP-API-1/27 was synthesized by catalytic reduction of 3,4-dihydroxybenzophenone in methanol for 6 h at ambient temperature, applying a hydrogen atmosphere and palladium/charcoal (10%). Purification was achieved by flash chromatography on silica with petrol ether/ethyl acetate (4:1) to yield a gray solid. $C_{13}H_{12}O_2$; MW 200,08; CAS [7005-43-8]; purity 97.5%; yield 90%; UV: λ_{max} = 285 nm.

Surface Plasmon Resonance Measurements—Solution competition assays based on surface plasmon resonance (SPR) were performed using streptavidin-coated sensor chips (GE Healthcare) to capture the N-terminally biotinylated peptide AKAP18δ-L314E, derived from the RII-binding domain of AKAP18δ (12). Binding of human PKA regulatory subunit RIIα or RIIβ to the AKAP18δ-L314E peptide surface and inhibition of RII binding by tested compounds were analyzed using a Biacore 3000 instrument (GE Healthcare) as described (17–19). Regulatory RIα subunits were captured on 8-AHA-cAMP surfaces, and association of an AKAP149 fragment (amino acids 285–387) encompassing its RI/RII-binding domain was investigated as described (19). Where indicated, RIα, RIβ, RIIα, and RIIβ were bound to 8-AHA-cAMP-coupled sensor chips as described (19). For direct binding studies, a Biacore S51 instrument (GE Healthcare) was used to monitor compound binding to immobilized RIIα. In brief, S CM-5 chips were used to immobilize 10000 RU of RIIα (20 μg/ml in 10 mM acetate pH 4.5) via standard amine coupling as recommended by the manufacturer. Interaction studies were performed in running buffer (25 mM Tris, pH 7.4, 150 mM NaCl, 50 μM EDTA, 5% DMSO, and 0.005% surfactant P20) at 25 °C. Nonspecific binding was subtracted using an *N*-hydroxysuccinimide (NHS)/ethyl-*N*-(3-diethylaminopropyl)carbodiimide (EDC) activated/deactivated blank surface, and a DMSO calibration procedure was performed to subtract artifacts caused by the solvent. FMP-API-1, FMP-API-1/27, Ht31, and combinations thereof were injected for 60 s at a flow rate of 30 μl/min, and the dissociation phase was monitored for 180 s. The surface was regenerated by a 30 s injection of 10 mM glycine, pH 9.5.

Nuclear Magnetic Resonance Measurements—All experiments were performed on a Bruker DRX600 spectrometer equipped with a *z* axis gradient 5-mm TXI Cryoprobe at 300 K. NMR samples of unlabeled RIIα (14 μM), GST-AKAP18δ, and ovalbumin (19 μM each) were prepared in 20 mM phos-

phate buffer (pH 7.4), and 1 mM FMP-API-1 in DMSO-d_6 was added to each. The final protein samples contained 2% DMSO-d_6. Saturation transfer difference (STD) NMR experiments were recorded with the carrier frequency set at 0.68 ppm for on-resonance irradiation and about 330 ppm for off-resonance irradiation. A train of 50 Gaussian-shaped pulses at 40 ms was applied, each separated by a 1-ms delay, for a total duration of 2.05 s, to achieve selective protein saturation. Acquisition of spectra was done with 32 scans and a relaxation delay of 1.3 s. A $T_{1\rho}$ spin-lock pulse of 40 ms was used to suppress the background protein signals. The STD spectrum was obtained from the internal subtraction of the on-resonance from the off-resonance data by phase cycling (20).

Preparation of Rat Neonatal and Adult Cardiac Myocytes—Neonatal cardiac myocytes were obtained from Wistar Kyoto (WKY) rats (1–2 days old). Primary cultures of adult cardiac myocytes from male WKY rats aged 3 months were performed as described previously (21).

Immunoprecipitation, cAMP-agarose Pull-down and RII Overlay Assays, Preparation of Cell Lysates, and Western Blotting—The experiments were carried out as described previously by us (17, 18, 22–24). AKAP150, phospho-phospholamban (both from Upstate), cardiac troponin I (c-TnI), c-TnI phosphorylated at $Ser^{23/24}$, PKA substrates phosphorylated by PKA at the consensus site RR*X*(S/T) (all from Cell Signaling Technology, Boston, MA), Yotiao (Novus Biologicals Inc., Littleton, CO), calsequestrin (GeneTex, San Antonio, TX), catalytic Cα, RIIα, and RIIβ subunits of PKA (BD Biosciences), and AKAP18δ (17) were detected by Western blot with specific primary and peroxidase-conjugated secondary antibodies. Immunoprecipitations of RII subunits and AKAP150 were carried out with the antibodies listed above. Signals were visualized using Lumi-Light Western blotting substrate solution and the Lumi Imager F1 (Roche Applied Science) (17). AKAPs were detected by RII overlay with ^{32}P-labeled recombinant RII subunits (17).

Cyclic AMP and Adenylyl Cyclase Assay—Radioimmunoassays were carried out to determine cAMP levels in rat neonatal cardiac myocytes as described (24). Cyclic AMP accumulations in uterine tissue samples were detected in the presence of the nonspecific phosphodiesterase inhibitor 3-isobutyl-1-methylxanthine by a competitive cAMP enzyme immunoassay kit. Adenylyl cyclase activity was assayed in HEK293 cells transiently expressing cyclic nucleotide-gated channels (CNGC) as cellular cAMP biosensors to measure changes in subplasmalemmal cAMP as described (25).

Kinase Activity Assays—The non-radioactive PepTag PKA assay (Promega, Madison, WI) was used to measure PKA activity from cell lysates and immunoprecipitates and to measure activity of recombinant catalytic subunits. The PepTag PKA assay is based on the phosphorylation of the fluorescent PKA substrate peptide, Leu-Arg-Arg-Ala-Ser-Leu-Gly (Kemptide) (PepTag A1 peptide), which, upon phosphorylation by PKA, acquires a negative charge and can be separated from the non-phosphorylated peptide by agarose gel electrophoresis.

To measure PKA activity in cell lysates, rat neonatal cardiac myocytes were plated onto 6-well tissue culture plates at a density of 2×10^6 cells/well. Myocytes were serum-starved overnight prior to the experiments, which were carried out 2 days after seeding. Small molecules, FMP-API-1 or FMP-API-1/27, were added to the medium as indicated in the figure legends. Cells were incubated for 30 min. Medium was removed, and cells were homogenized in 100 μl/well lysis buffer (10 mM K_2HPO_4, 150 mM NaCl, 5 mM EDTA, 5 mM EGTA, 1% Triton X-100, 0.25% deoxycholate, 1 mM benzamidine, 0.5 mM phenylmethanesulfonyl fluoride, 3.2 μg/ml trypsin inhibitor I-S, 1.4 μg/ml aprotinin). The lysates were cleared by centrifugation (12,000 $\times$ *g*, 4 °C, 10 min). The supernatants were assayed for PKA activity in the absence of added cAMP. PepTag A1 peptide (0.056 μg/μl) was incubated with 15 μl of the supernatant in PepTag PKA reaction buffer (final volume 25 μl) at 30 °C for 10 min. The reaction was stopped by boiling the samples for 10 min. Phosphorylated and non-phosphorylated PepTag A1 peptides were separated by 0.8% agarose gel electrophoresis. Fluorescence was recorded with the Lumi Imager F1 (Roche Applied Science), and bands were analyzed by densitometry.

To measure PKA activity in AKAP150-immunoprecipitates, AKAP150 was immunoprecipitated as described (17). Protein A-Sepharose beads were resuspended in 100 μl of lysis buffer, and 14.3-μl bead suspensions were incubated with PepTag A1 peptide (0.056 μg/μl), and 5 μl of PKA activator solution (cAMP) in PepTag PKA reaction buffer (final volume 25 μl) at 30 °C for 10 min. The assay was continued as described above.

To measure the activity of PKA catalytic subunits *in vitro*, 5 μl of recombinant catalytic subunits (0.0167 mg/ml) were incubated with PepTag A1 peptide (0.056 μg/μl) in PepTag PKA reaction buffer (final volume 25 μl) at 30 °C for 10 min with or without 0.013 mg/ml recombinant RII subunits or 0.04 μM cAMP or FMP-API-1 as indicated in the figure legends. The assay was continued as described above.

The effect of FMP-API-1 (100 μM) on ErbB1, MEK1, ERK1 and -2, ROCK1 and -2, PKCα, CaMKIIα, and GSK3β activities was assayed using Invitrogen's SelectScreen commercial profiling service.

Phosphatase and PDE4 Activity Assays—Calcineurin was assayed using the Calcineurin Cellular Assay Kit Plus from Biomol GmbH (Hamburg, Germany) according to the manufacturer's instructions. For analysis of neonatal rat cardiac myocyte cell lysates, cells were seeded in 6-well plates (2×10^6 cells/well), cultured for 24 h, and treated with DMSO (1%) or FMP-API-1 (in the indicated concentrations, 30 min). After washing three times with TBS, cells were detached from the wells with a cell scraper and suspended in ice-cold lysis buffer (270 μl). Samples were centrifuged (10 min, 22,000 $\times$ *g*, 4 °C), and activities of Ca^{2+}-independent phosphatases and calcineurin were assessed. To measure the specific influence of FMP-API-1 on calcineurin, the recombinant enzyme included in the kit was diluted 1:6.25 in lysis buffer, and FMP-API-1 was added. PDE4 activities were measured using 20 μg of protein, in 25 μl of cell lysates prepared from neonatal cardiac myocytes as described (24).

Electrophysiology—Whole-cell L-type I_{Ca} (Ca^{2+} current) was recorded from rat neonatal cardiac myocytes (see

above) as described previously (16). For measurements of I_{Ks} channel currents, COSM7 cells were utilized as described (26, 27).

Contractility of Isolated Perfused Heart Preparations—Hearts were obtained from WKY rats (12-week-old males) and subjected to Langendorff heart experiments as described (28).

In Vitro Uterus Contractility Studies—All experiments involving animal subjects were carried out with the approval of the Hungarian Ethical Committee for Animal Research (registration number IV/01758-2/2008) and under the control of the ISO-9001:2008 Quality Management System. Sexually mature female Sprague-Dawley rats (body mass 140–160 g,

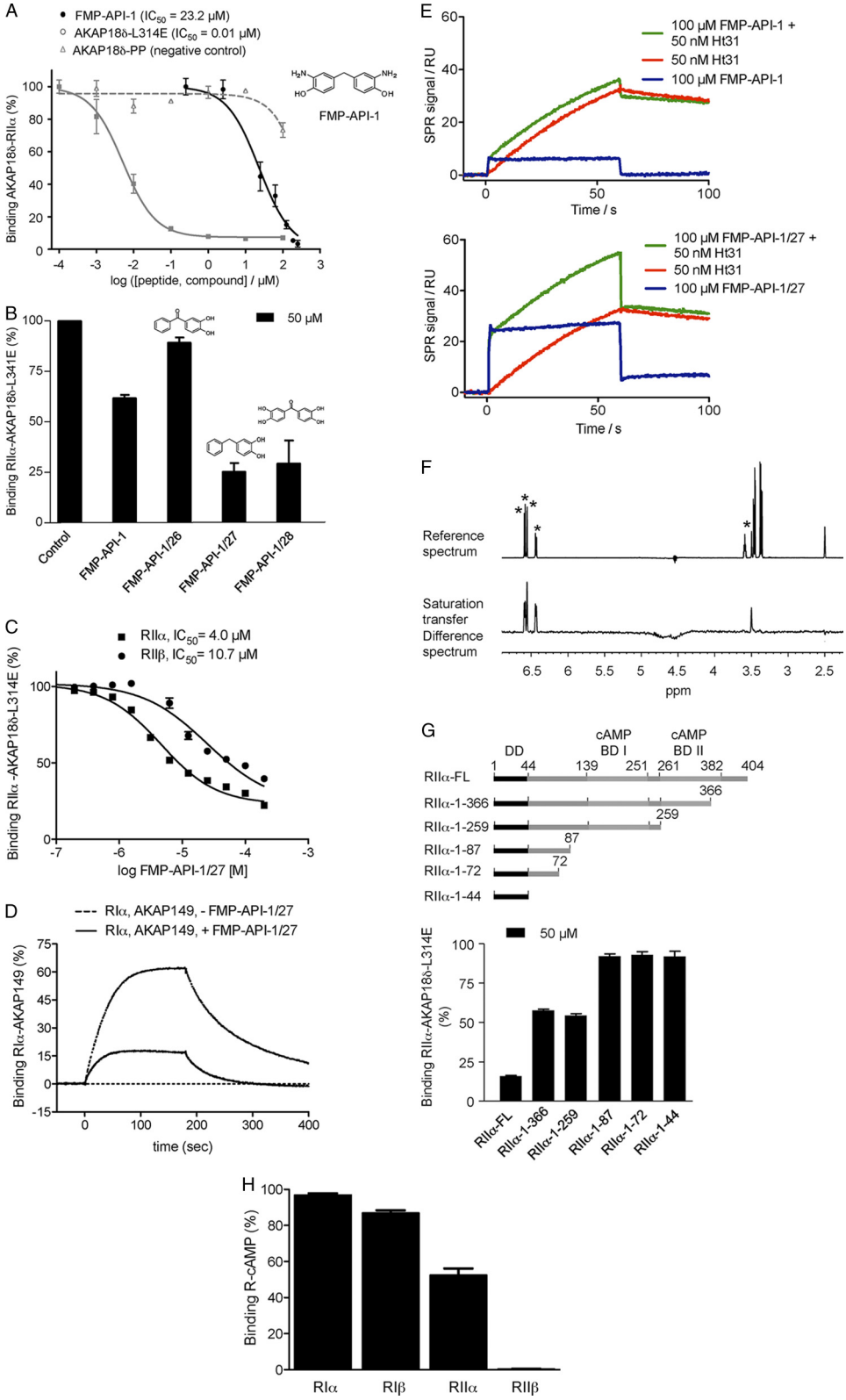

50–60 days old) were mated in the early morning hours. Copulation was confirmed by the presence of a copulation plug or spermatozoa in the vagina. The day of copulation was considered to be the first day of pregnancy.

On day 22 of pregnancy, the rats were sacrificed (CO_2 inhalation), and the uteri were removed and prepared for the *in vitro* contractility assay. The isolated uterine horns were immediately placed in an organ bath (de Jongh solution; containing 137 mM NaCl, 3 mM KCl, 1 mM $CaCl_2$, 1 mM $MgCl_2$, 12 mM $NaHCO_3$, 4 mM Na_2HPO_4, 6 mM glucose, pH 7.4) perfused with 95% oxygen and 5% carbon dioxide. They were trimmed of fat, and the feto-placental units were removed. Temperature was maintained at 37 °C. Four rings 1 cm long were sliced from the middle part of each horn, including implantation sites, and tested in parallel. They were mounted vertically between two platinum electrodes in the above-mentioned organ bath under the same conditions. After mounting, the initial tension was set at 1.5 g, and the rings were equilibrated for 60 min. Then rhythmic contractions were elicited by 25 mM KCl. The tension of the myometrial rings was measured with a strain gauge transducer (SG-02, Experimetria Ltd., Budapest, Hungary), recorded, and analyzed by the SPEL advanced ISOSYS data acquisition system (Experimetria Ltd.). Areas under the curves of 4-min periods of each concentration were evaluated. The maximal contraction-inhibiting values were calculated with the Prism 4.0 computer program (GraphPad Inc., San Diego, CA).

Statistics—One-way analysis of variance, Dunnett's multiple comparison test, and single- and double-tailed Student's *t* test were carried out for statistical analyses as indicated.

RESULTS

FMP-API-1 Inhibits AKAP-PKA Interactions by Allosteric Non-covalent Binding to Regulatory Subunits of PKA—In order to identify small molecules disrupting AKAP-PKA interactions, we developed an ELISA-based screening assay, where full-length AKAP18δ was added to RIIα subunits of PKA bound to 384-well microtiter plates. Interaction was detected using primary antibodies specific for AKAP18δ, secondary peroxidase-conjugated antibodies, and a chemiluminescent peroxidase substrate (Fig. 1*A*) (12). The assay was validated using the PKA anchoring disruptor peptide, AKAP18δ-L314E, derived from the RII-binding domain of AKAP18δ (12). This peptide inhibited the AKAP18δ-RIIα subunit interaction with an IC_{50} value of 10 nM, whereas the inactive control peptide AKAP18δ-PP did not affect the interaction in concentrations of up to 1 mM (Fig. 1*A*). Using this assay system, 20,000 small molecules were screened (FMP small molecule library FMP_20,000). The molecules possess an average molecular mass of 250 Da and were selected on the basis of a large chemical diversity. They have druglike properties in that they fulfill the Lipinski rules to increase bioavailability (29). Nine compounds were identified as potential disruptors of the AKAP18δ-RIIα subunit interaction.

The most promising candidate, compound FMP-API-1 (IC_{50} = 23.3 μM; Fig. 1*A*), was selected for validation in a secondary assay, SPR measurements. In the SPR measurements, the peptide AKAP18δ-L314E was immobilized on the chip surface, and recombinant RIIα subunits preincubated with FMP-API-1 (50 μM) were added. FMP-API-1 inhibited the interaction by ~40% (Fig. 1*B*).

For initial structure-activity relationship investigations, a focused library of 26 derivatives of FMP-API-1 was synthesized (Table 1). SPR measurements revealed that only derivatives FMP-API-1/27 and FMP-API-1/28 disrupted the interaction of the peptide AKAP18δ-L314E with RIIα subunits effectively. At a concentration of 50 μM, FMP-API-1/27 and FMP-API-1/28 inhibited the interaction of RII subunits with the peptide by 75 and 70%, respectively (Fig. 1*B*). Titrations revealed that FMP-API-1/27 inhibited the interaction of RIIα subunits with the peptide AKAP-18δ-L314E with IC_{50} = 4.0 ± 0.1 μM (Fig. 1*C*). In contrast to FMP-API-1, neither FMP-API-1/27 nor FMP-API-1/28 contains any amino groups, suggesting that these groups are not involved in the interaction with the target protein, leading to inhibition of the interaction. In addition, the structure of FMP-API-1/28 suggests that the addition of a keto function to the central methylene group connecting the two aromatic systems does not impair the activity. Thus, possible steric hindrance caused by the keto function or the decreased flexibility in the center of the active pharmacophore apparently did not interfere with

FIGURE 1. **FMP-API-1 inhibits the interaction between AKAP18δ and RIIα by allosteric binding to the RII subunits.** *A*, microtiter plates were coated with RIIα (15 ng/well) and incubated with AKAP18δ (15 ng/well) in the presence of the PKA anchoring disruptor peptide AKAP18δ-L314E, the inactive control peptide AKAP18δ-PP, or FMP-API-1 in the indicated concentrations (12). Binding of AKAP18δ to RIIα was detected by incubation with primary anti-AKAP18δ (A18δ4 antibody (17)) and secondary peroxidase-coupled antibodies and subsequently with a chemiluminescence peroxidase substrate solution. Signals were recorded in a luminescence intensity reader ($n = 5$; shown are means ± S.E. (*error bars*)). AKAP18δ-L314E and AKAP18δ-PP curves are significantly different ($p < 0.01$), and the FMP-API-1 inhibition curve is significantly different from the control (DMSO) ($p < 0.05$). The structure shows FMP-API-1. *B*, SPR measurements confirming the inhibitory effect of FMP-API-1 and its derivatives FMP-API-1/26, -27, and -28. The peptide AKAP18δ-L314E was coupled to sensor chip surfaces, and RIIα (500 nM), preincubated with the small molecules (50 μM), was added. As a control, the small molecules were omitted. Shown are means from two independent experiments. *C*, FMP-API-1 inhibits the interactions between regulatory RIIα and RIIβ subunits of PKA with the peptide AKAP18δ-L314E. The peptide was coupled to SPR sensor chips, and RIIα and RIIβ, preincubated with FMP-API-1/27 (391 nM to 200 μM), were added to determine the IC_{50} values for the inhibitory effect of the molecule. Shown are means from two independent experiments. *D*, 8-AHA-cAMP was coupled to SPR sensor chips, and RIα subunits were captured on the surface. AKAP149 was added in the absence or presence of FMP-API-1/27. Shown is the result of one of two independent experiments. *E*, the peptide Ht31 and the small molecules FMP-API-1 and FMP-API-1/27 bind additively to RIIα. Association and dissociation of the small molecules (100 μM) and Ht31 (50 nM), either alone or in the indicated combination, were measured by SPR using a sensor chip coated with full-length RIIα. Shown are means from two independent experiments. *F*, FMP-API-1 binds to full-length PKA RIIα. *Top*, reference NMR spectrum of FMP-API-1 (1 mM) in the presence of RIIα (14 μM). *Asterisks* indicate the proton signals of the compound. *Bottom*, STD NMR spectrum of FMP-API-1 (1 mM) in the presence of RIIα (14 μM). Shown are representative spectra from three independent experiments. *G*, the indicated versions of RIIα were generated and preincubated with the FMP-API-1 derivative FMP-API-1/27 (50 μM), and binding to the peptide AKAP18δ-L314E was assessed by SPR measurements as described in *B* and *C*. Shown are means from two independent experiments. *H*, 8-AHA-cAMP was coupled to SPR sensor chips, and regulatory subunits of PKA (RIα, RIβ, RIIα, and RIIβ), preincubated with FMP-API-1/27 (50 μM), were added. Shown are means from two independent experiments.

TABLE 1
Focused library of FMP-API-1 derivatives

Compound FMP-API-1	Name	Formula	MW	CAS
FMP-API-1	3,3'-Diamino-4,4'-dihydroxydiphenylmethane	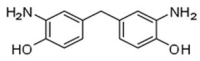 $C_{13}H_{14}N_2O_2$	230,3	16523-28-7
/03	4,4'-Oxybis(2-aminophenol)	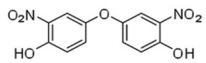 $C_{12}H_{12}N_2O_2$	216,2	6423-17-2
/04	3,3'-Methylenebis(6-aminophenol) 3,3'-Dihydroxy-4,4'-diaminodiphenylmethane 4,4'-Diamino-3,3'-dihydroxydiphenylmethane	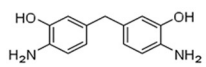 $C_{13}H_{14}N_2O_2$	230,3	22428-30-4
/05	Bis-(4-amino-3,5-dimethylphenyl)-methane 4,4′-Methylenebis(2,6-dimethylaniline)	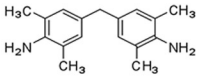 $C_{17}H_{22}N_2$	254,4	4073-98-7
/06	Bis-(3-aminophenyl)-methane 3,3′- Methylenedianiline	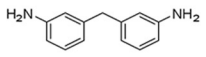 $C_{13}H_{14}N_2$	198,3	19471-12-6
/07	Bis-(3,5-di-tert.-butyl-4-hydroxyphenyl) Methylenebis(2,6-di-tert-butylphenol) 4,4′-	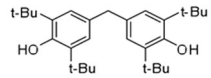 $C_{29}H_{44}O_2$	424,7	118-82-1
/08	1,1-Bis-(4-hydroxyphenyl)-ethane 4,4′- Ethylidenebisphenol	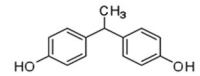 $C_{14}H_{14}O_2$	214,3	2081-08-5
/09	Bis-(4-hydroxyphenyl)-methan	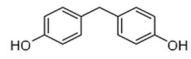 $C_{13}H_{12}O_2$	200,2	620-92-8
/10	2,2-Bis-(3-amino-4-hydroxyphenyl)hexa- fluoropropane	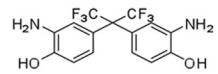 $C_{15}H_{12}F_6N_2O_2$	366,3	83558-87-6
/11	4,4'-Dichlorobenzhydrol	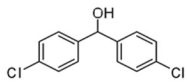 $C_{13}H_{10}Cl_20$	253,1	90-97-1
/12	4-Acetamidofluorene	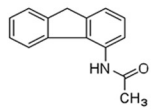 $C_{15}H_{13}NO$	223,3	28322-02-3
/14	4-Hydroxy-3-nitro-benzophenone	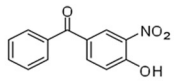 $C_{13}H_9NO_4$	243,2	5464-98-2
/16	3-Amino-4,4'-dihydroxydiphenylmethane	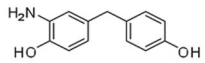 $C_{13}H_{13}NO_2$	215,3	pending
/20	1,1-Bis-(3-Amino-4-hydroxyphenyl)-ethane	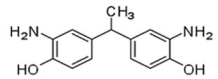 $C_{14}H_{16}N_2O_2$	244,3	pending
/21	3-Amino-1,1-bis-(4-hydroxyphenyl)-ethane	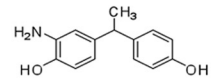 $C_{14}H_{15}NO_2$	229,3	pending
/23	Bis-(4-hydroxy-3,5-bishydroxymethylphenyl)methane	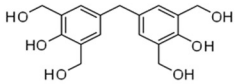 $C_{17}H_{20}O_6$	320,3	13653-12-8
/25	3-Amino-4-hydroxy-benzophenone	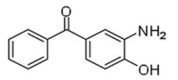 $C_{13}H_{11}NO_2$	213,23	42404-41-1
/26	3,4-Dihydroxy-benzophenone	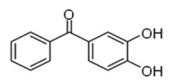 $C_{13}H_{10}O_3$	214,22	10425-11-3

TABLE 1—*continued*

Compound FMP-API-1	Name	Formula		MW	CAS
/27	4-Benzyl-pyrocatechol	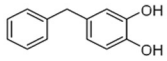	$C_{13}H_{12}O_2$	200,08	7005-43-8
/28	Bis-(3,4-dihydroxy-phenyl)-methanone	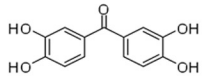	$C_{13}H_{10}O_5$	246,05	61445-49-6
/30	Bis-(3-amino-4-hydroxy-phenyl)-methane	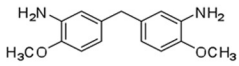	$C_{15}H_{18}N_2O_2$	258,32	23186-90-5
/32	3,4-Bis-(3-amino-4-hydroxy-phenyl)-hexane	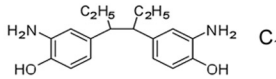	$C_{18}H_{24}N_2O_2$	300,4	41172-52-5 66877-41-6
/33	4,4'-Diaminobibenzyl	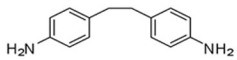	$C_{14}H_{16}N_2$	212,29	621-95-4
/34	Desoxy-4-anisoin	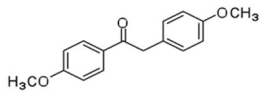	$C_{16}H_{16}O_3$	256,3	120-44-5
/35	4, 4'-Dimethoxybibenzyl	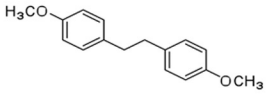	$C_{16}H_{18}O_2$	242,31	1657-55-2
/38	3,3'-Diamino-4,4'-dihydroxybibenzyl	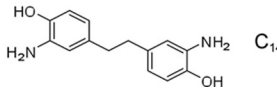	$C_{14}H_{16}N_2O_2$	244,29	pending

the interaction. Removal of the two hydroxyl groups in the 3- and 4-positions from one of the aromatic systems of FMP-API-1/28, yielding FMP-API-1/26, abolished the inhibitory action of FMP-API-1/28. The structure of the inactive compound FMP-API-1/30, possessing methoxy (-OCH_3) and amino (-NH_2) groups instead of hydroxyl (-OH) groups, confirms that the hydroxyl groups are relevant for the inhibitory effect of the molecules. It is possible that the hydroxyl groups serve as hydrogen bond donors, facilitating the interaction of the compound with hydrogen bond acceptors in the target protein.

Due to the similarity between RIIα and RIIβ subunits, the interactions between both subunits and AKAPs may be inhibited by the small molecules. Therefore, SPR experiments, set up as described above, were also used to quantitatively determine the inhibitory effects of FMP-API-1/27 on the interaction of RIIβ subunits with the AKAP18δ-derived peptides. Fig. 1*C* shows that FMP-API-1/27 inhibits the interactions with $IC_{50} = 10.7 \pm 1.8$ μM, suggesting that the molecule has similar effects on RIIα- and RIIβ-AKAP interactions. A different SPR experiment was established for investigating the effect of FMP-API-1/27 on regulatory RI subunit interactions with AKAPs. RIα subunits were captured on 8-AHA-cAMP sensor chip surfaces, and a fragment of the dual specificity AKAP, D-AKAP1 (AKAP149) encompassing the RI/RII interacting domain (amino acids 285–387) (30) was allowed to bind to the RIα subunits in the absence or presence of FMP-API-1/27. The small molecule inhibits the interaction by around 75% (Fig. 1*D*). RIβ cannot be tested in this setup because it does not bind to D-AKAP1 (19). Thus, the small molecules inhibit both RI and RII interactions with AKAPs. The following exemplary experiments were carried out with RIIα subunits.

With the AKAP18δ-derived peptides coupled to the Biacore sensor chips, the SPR experiments (Fig. 1, *B* and *D*) were designed in such a way that the small molecules require either interference with the interacting surfaces or allosteric binding to RII subunits to inhibit the interaction. In order to investigate whether the small molecules act through interference with the interacting domains, SPR sensor chips were coated with full-length RIIα, and the association and dissociation of FMP-API-1, FMP-API-1/27, and Ht31 or each small molecule combined with the peptide was measured (Fig. 1*E*). The additive association curve resulting from the combination of small molecule and peptide suggests binding of the small molecules to an allosteric site on RIIα rather than to the D/D domain. In addition, the additive binding of the PKA disruptor peptide Ht31 along with FMP-API-1 would not be observed if the small molecule interfered with R subunit dimerization because this is required for AKAP binding. In line with these observations, the D/D domain coupled to an SPR sensor chip did not bind the small molecules (data not shown), and $^{1}H,^{15}N$ HSQC NMR experiments with ^{15}N-labeled RIIα D/D domain (residues 1–44) showed no binding of FMP-API-1 (0.1–2 mM; supplemental Fig. 1).

To confirm that the inhibitory effect is mediated by binding of the molecules to the R subunits, NMR STD experiments (20) were performed with FMP-API-1 and full-length RII subunits (Fig. 1*F*). A reference proton spectrum of FMP-API-1 and a STD spectrum of the full-length PKA RIIα-FMP-API-1

sample were recorded (Fig. 1*F*). The resonance signals of FMP-API-1 in the STD spectrum indicated binding of the compound to the full-length RIIα subunit. Binding of FMP-API-1 to an unrelated protein, ovalbumin, was not observed (data not shown). Binding of FMP-API-1 to the full-length RIIα subunit is noncovalent and reversible (Fig. 1*F*). This can be concluded from the STD NMR experiments, which generally detect reversible interactions (20). If the binding were covalent, the line width of the small molecule signals would change drastically. Additional support for non-covalent binding of FMP-API-1 to RIIα subunits stems from mass spectrometric analyses of recombinant RIIα subunits after incubation with the compound (2 h, room temperature). In these experiments, FMP-API-1-modified amino acids within RIIα subunits were not detected (data not shown).

Further confirmation that the binding site of FMP-API-1/27 in RIIα subunits is located C-terminal to the D/D domain stems from SPR experiments using the truncations of RIIα indicated in Fig. 1*G*. In these experiments, FMP-API-1/27 (50 μM) was preincubated with the full-length RIIα or the truncations. The molecule reduced the binding of full-length RIIα subunits (amino acids 1–404) to the AKAP18δ-derived peptides coupled to the sensor chips to ~15–20%. Consistent with the data illustrated in Fig. 1*E* and supplemental Fig. 1, it did not affect the interaction of the peptide with the D/D domain (RIIα 1–44) or extended versions thereof (RIIα 1–44, 1–72, and 1–87). Further elongation to amino acid 366 (constructs RIIα 1–259 and RIIα 1–366) impaired the inhibitory effect of the compound to the peptides on the sensor chips (reduction in binding to 60–70%). STD NMR experiments showed that the observed inhibition was due to direct binding of FMP-API-1 to the relevant RIIα truncates because binding was detected for RIIα 1–259 and RIIα 1–366, but not for RIIα 1–44, RIIα 1–72, and RIIα 1–87 (data not shown). A shorter construct (RIIα 1–156) proved to be unfolded in STD NMR experiments. Its interaction with the small molecules could therefore not be evaluated in SPR (Fig. 1*G*) or STD NMR experiments.

Next, we investigated whether the interaction of FMP-API-1 with a region C-terminal of the D/D domain interferes with the interaction of the regulatory subunits with cAMP (Fig. 1*H*). Regulatory subunits were preincubated with FMP-API-1/27 and captured on 8-AHA-cAMP sensor chips. This experiment revealed that FMP-API-1/27 hardly affected binding of the RIα and -β subunits to cAMP. In contrast, binding of RIIα to cAMP was reduced by 50%, and that of RIIβ subunits was reduced by >90%. The inhibitory effect of the molecules on the interaction of RII subunits with cAMP was confirmed in cAMP-agarose precipitation experiments (Fig. 2*B*). However, this revealed that in cells, this effect was far less pronounced because around 75% of RIIβ could be precipitated in the presence of FMP-API-1 compared with control.

Collectively, the data indicate that FMP-API-1/27 binds C-terminally from the D/D domain. This region of regulatory subunits is apparently also crucial for the binding of AKAPs. The region between amino acids 88 and 156 encompasses the autoinhibitory domain of PKA that is involved in the inhibition of catalytic subunits in the holoenzyme. Targeting a region involving the autoinhibitory domain with small molecules may not only displace RII subunits from AKAPs but may also modulate the activity of PKA. Indeed, as we show below, both FMP-API-1 and FMP-API-1/27 activate the kinase (Fig. 3 and supplemental Fig. 2*A*).

FMP-API-1 and FMP-API-1/27 Disrupt AKAP-PKA Interactions in Cardiac Myocytes—The effect of FMP-API-1 on AKAP-PKA interactions in a cellular environment was investigated in rat neonatal cardiac myocytes. Initially, immunoprecipitation experiments were performed (Fig. 2*A*). AKAP150 was immunoprecipitated from cells left untreated or treated with FMP-API-1 (300 μM), isoproterenol (ISO; 100 nM), or a combination of the two. Immunoprecipitation of AKAP150 was confirmed by Western blotting (Fig. 2*A*, *top*). Compared with the precipitates obtained with preimmune serum, AKAP150 was strongly enriched in precipitates obtained with specific anti-AKAP150 antibodies. If FMP-API-1 displaced PKA from AKAPs, immunoprecipitates from FMP-API-1-treated cells are expected to contain less PKA activity than precipitates from untreated cells. Indeed, immunoprecipitates from cells treated with FMP-API-1 contained significantly less PKA activity than those from untreated cells (Fig. 2*A*). Isoproterenol induces PKA activation (*i.e.* release of catalytic subunits from R subunits). Fig. 2*A* shows that ISO consistently caused a weak decrease in PKA activity in the precipitates. FMP-API-1 decreased the AKAP150-associated PKA activity to a significantly larger degree. This effect was not further enhanced if FMP-API-1 was combined with isoproterenol.

Additionally, the effect of FMP-API-1 on AKAP-PKA interactions in neonatal cardiac myocytes was investigated in cAMP-agarose precipitation experiments. The cells were treated with FMP-API-1 (100 μM) and lysed, and a cAMP-agarose precipitation assay was performed. Cyclic AMP-agarose retains regulatory subunits of PKA, including associated binding proteins, such as AKAPs. Western blot analysis of cAMP-agarose eluates revealed that consistently fewer RIIβ subunits were recovered in the presence of FMP-API-1 (Fig. 2*B*). However, the difference between the amount of RIIβ precipitates and the amount of RIIβ precipitates obtained from untreated controls was not significant. The less pronounced inhibitory effect of FMP-API-1/27 on the interaction of RII subunits with the cAMP on the agarose compared with the interaction with cAMP on SPR sensor chips (Fig. 1*H*) may be explained by differences in the experimental setups. In the SPR experiments, the interaction of RII subunits with cAMP occurs under flow, which may impair a transient interaction of RII with cAMP and lead to a significant decrease in RII binding to cAMP. In the cAMP-agarose experiment, the cells are incubated with the compound for 30 min. The cells are lysed, and the lysates are incubated with cAMP-agarose overnight in the presence of FMP-API-1. Compared with the SPR setup, we deem the results from the cAMP-agarose precipitations to be physiologically more similar to the cellular systems used to characterize FMP-API-1 (see below). The amounts of several AKAPs precipitated with the cAMP-agarose were significantly reduced, whereby the amounts of AKAP18δ, AKAP150, and AKAP Yotiao were reduced to a lower degree

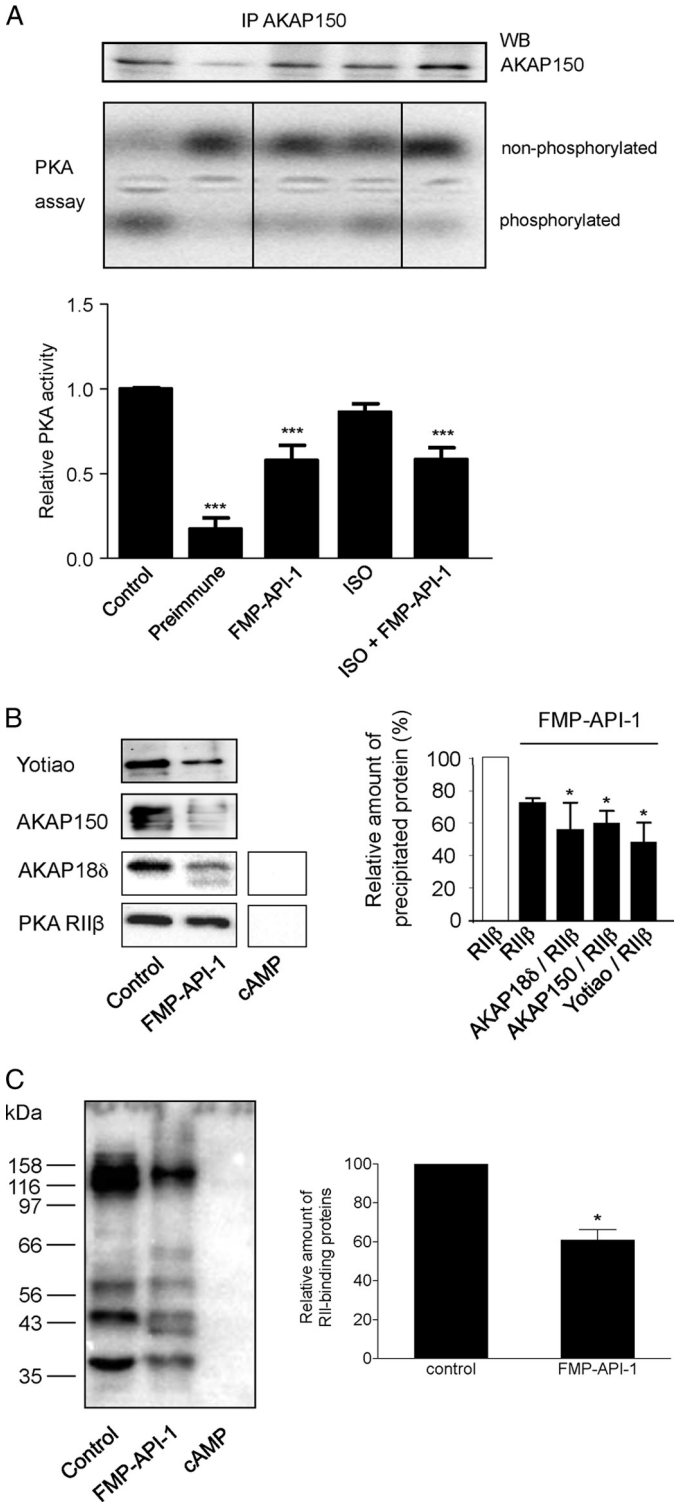

FIGURE 2. **FMP-API-1 disrupts AKAP-PKA interactions in cardiac myocytes.** *A*, rat neonatal cardiac myocytes were treated with FMP-API-1 (300 μM) or ISO (100 nM) either alone or in combination (*FMP-API-1 + ISO*). DMSO-treated (0.1%) cells served as control. Immunoprecipitation (*IP*) was performed with anti-AKAP150 antibody or preimmune serum as a negative control (*top*). *WB*, Western blot. *Middle*, agarose gel from a representative experiment showing PepTag A1 peptide phosphorylation by PKA co-immunoprecipitated with AKAP150. *Bottom*, the amounts of phosphorylated and non-phosphorylated PepTag A1 peptides were densitometrically evaluated, and the ratio was calculated. PKA activity in the precipitates is expressed as the ratio of phosphorylated to non-phosphorylated PepTag A1 peptides. Values are mean ± S.E. (*error bars*); ***, significantly different from controls ($p = 0.001$; $n \geq 7$ independent experiments for each condition). *B*, *left*, cAMP-agarose precipitates were obtained from rat neonatal cardiac myocytes treated with FMP-API-1 (100 μM) or the FMP-API-1 solvent DMSO (0.1%; control). As a control, excessive cAMP (50 mM) was added to lysates obtained from control cells. This prevents binding of regulatory PKA subunits to cAMP-agarose and thereby precipitation of AKAPs. RIIβ, Yotiao, AKAP150, and AKAP18δ were detected by Western blotting. *Right*, semiquantitative evaluation of the Western blots shown on the *left*. Signal intensities were densitometrically determined. Shown is the relative amount of RIIβ subunits precipitated in the absence or presence of FMP-API-1 and the ratios of AKAPs/RIIβ. *, $p < 0.05$, statistically significant difference *versus* RIIβ. *C*, *left*, detection of AKAPs in cAMP-agarose precipitates (obtained as described in *B*) by RII overlay assay. Proteins were separated by SDS-PAGE, blotted onto filters, and overlaid with ^{32}P-labeled RII subunits of PKA. Binding is detected by autoradiography. Shown are representative results from three independent experiments. *Right*, semiquantitative evaluation of the autoradiographs shown on the *left*. Signal intensities of all bands in each lane were densitometrically determined. *, $p < 0.05$.

than explained by the lower amount of RII subunits precipitated in the presence of the small molecule. The data indicate that FMP-API-1 inhibits AKAP-PKA interactions in cells (Fig. 2*B*). For the simultaneous detection of all AKAPs in the cAMP-agarose precipitates, an RII overlay assay was applied. This assay detected various RII-binding proteins in cAMP-agarose precipitates obtained from untreated cells. Consistent with the Western blot shown in Fig. 2*A*, in precipitates obtained from cells treated with FMP-API-1, the signals were significantly reduced (Fig. 2*C*). As expected, in the presence of excess cAMP, the cAMP-agarose did not recover detectable amounts of RII-binding proteins.

Taken together, these experiments show that FMP-API-1 and FMP-API-1/27 inhibit the interaction of endogenous AKAPs with PKA *in vitro* and in cultured cells *in vivo*. In addition, the data underline that the molecule is membrane-permeable, as predicted from its compliance with the Lipinski rules (29).

FMP-API-1 Activates PKA but Not Other Kinases—The binding region of FMP-API-1 may involve the autoinhibitory region and/or the nucleotide binding regions of regulatory subunits (Fig. 1, *F–H*). Thus, FMP-API-1 might also modulate PKA activity. To test this hypothesis, an *in vitro* PKA activity assay was performed (Fig. 3*A*). RII subunits bind to the catalytic subunits and potently inhibit their activity. cAMP causes the dissociation of C subunits from RII subunits and thereby activation of the catalytic subunits. RIIα subunits were titrated to catalytic subunits to limit catalytic subunit activity to ~40% (Fig. 3*A*, *left*). The addition of either cAMP (5 μM) or FMP-API-1 (100 μM and 1 mM) induced an increase in the activity of the catalytic subunits in the presence of RII subunits, suggesting that FMP-API-1 binding to regulatory subunits (Fig. 1) dissociates catalytic from regulatory subunits. The effect of FMP-API-1 on the interaction of RII and C subunits was also tested in precipitation assays using HEK293 cells and neonatal cardiac myocytes. RIIβ subunits were immunoprecipitated from untreated cells and cells preincubated with FMP-API-1 (100 μM), and co-immunoprecipitated Cα subunits were detected by Western blotting (Fig. 3*B*). The presence of FMP-API-1 reduced the amount of co-immunoprecipitated C subunits in both cell types (Fig. 3*A* shows a representative experiment using HEK293 cells). This is in line with the activation of PKA observed *in vitro*. To further test

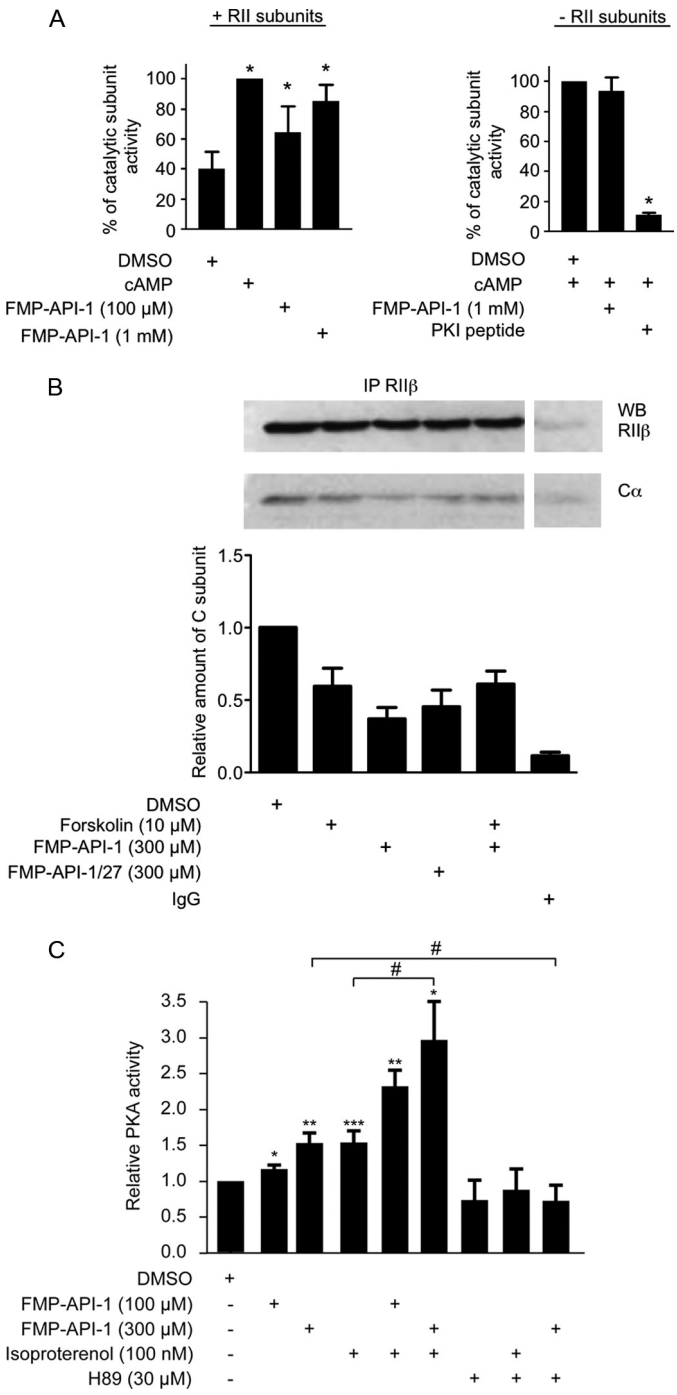

FIGURE 3. **FMP-API-1 activates PKA.** *A*, *left*, recombinant RIIα (0.013 ng) and catalytic subunits (0.0167 mg/ml) of PKA were incubated with DMSO (0.1%), the solvent of FMP-API-1 as a control, and cAMP and/or FMP-API-1 as indicated, and PKA activity was assessed using the PepTag A1 peptide phosphorylation assay as described in the legend to Fig. 2 (mean ± S.E. (*error bars*), three independent experiments). *, $p < 0.05$ statistically significant difference *versus* DMSO. *Right*, recombinant catalytic subunits alone were incubated with DMSO (0.1%), FMP-API-1, or the specific PKA inhibitor peptide (protein kinase inhibitor; *PKI*) as indicated, and PKA activity was assessed (mean ± S.E., three independent experiments). *, $p < 0.05$; **, $p < 0.005$ statistically significant difference *versus* DMSO. *B*, *top*, HEK293 cells were incubated with FMP-API-1 (100 or 300 μM) for 30 min. RIIα subunits were immunoprecipitated (*IP*), and co-immunoprecipitated catalytic Cα subunits of PKA were detected by Western blotting (*WB*). *Bottom*, semiquantitative evaluation of the Western blot shown in the *top*. The signal intensities were densitometrically determined. Shown are means from two independent experiments. *C*, rat neonatal cardiac myocytes were treated with DMSO (0.1%) as a control, FMP-API-1, isoproterenol, H89, or the indicated combinations of agents. Cell lysates were prepared and cleared by centrifugation, and PKA activity in the supernatants was assessed (mean ± S.E., three independent experiments). *, $p < 0.05$; **, $p < 0.005$; ***, $p < 0.001$, statistically significant difference *versus* DMSO. #, $p < 0.05$ as indicated.

whether FMP-API-1 increases PKA activity in cells, cardiac myocytes were incubated with FMP-API-1, the cells were lysed, lysates were cleared from cell debris, and PKA activity was measured. Fig. 3*C* shows that 100 μM FMP-API-1 activated PKA and that 300 μM FMP-API-1 increased PKA activity to a level similar to that reached if the cells had been treated with isoproterenol (100 nM). In combination, FMP-API-1 and isoproterenol acted additively. Both the FMP-API-1- and isoproterenol-induced activity increases were prevented with the PKA inhibitor, H89.

Further *in vitro* kinase assays investigated whether high concentrations of FMP-API-1 affected catalytic subunit activity in the absence of regulatory subunits. The activity of catalytic subunits of PKA was not even affected by concentrations of FMP-API-1 as high as 1 mM, whereas the specific inhibitor peptide derived from the heat-stable protein kinase inhibitor fully blocked catalytic subunit activity (Fig. 3*A*, *right*). FMP-API-1 (100 μM) did not activate in *in vitro* kinase assays ErbB1, MEK1, ERK1 and -2, ROCK1 and -2, PKCα, CaMKIIα, and GSK3β (supplemental Fig. 3). Indeed, these kinases were inhibited to a minor extent ~10–17%, whereas CaMKIIα and GSK3β were somewhat more sensitive to the compound (they were inhibited by 36 and 25%, respectively; supplemental Fig. 3). We have chosen these kinases because they are involved in controlling cardiac myocyte functions, including contractility.

FMP-API-1 Inhibits β-Adrenoreceptor-mediated Increases of L-type Ca^{2+}- and I_{Ks} K^+ Channel Currents—Functional consequences of the disruption of AKAP-PKA interactions in rat neonatal cardiac myocytes were examined by whole-cell patch clamp experiments. β-Adrenoreceptor stimulation causes enhanced Ca^{2+} entry into cardiac myocytes through PKA phosphorylation of L-type Ca^{2+} channels. The phosphorylation is facilitated by AKAP18α tethering PKA to the channel (31). Fig. 4*A* depicts patch clamp experiments using rat neonatal cardiac myocytes. These show that FMP-API-1 (100 μM), applied through the patch pipette, abolished Ca^{2+} current increases stimulated by the β-adrenergic agonist ISO (100 nM). The inhibitory effect of FMP-API-1 was similar to that achieved using the PKA anchoring disruptor peptide AKAP18δ-L314E (12). FMP-API-1 (100 μM) did not inhibit L-type Ca^{2+} currents stimulated by the channel activator Bay K 8644, indicating that FMP-API-1 does not interfere with the channels but rather disrupts the AKAP18α-PKA interaction.

The AKAP Yotiao tethers PKA to I_{Ks} K^+ channels and thereby facilitates channel phosphorylation by PKA (32). In order to test whether the observed inhibition of the Yotiao-PKA interaction by FMP-API-1 (Fig. 2*B*) prevents β-adrenoreceptor-induced increases in I_{Ks} currents, whole-cell patch clamp experiments were carried out (Fig. 4*B*). I_{Ks} K^+ channel currents are not detectable in neonatal cardiac myocytes. Therefore, the pore-forming channel subunit KCNQ1 and its

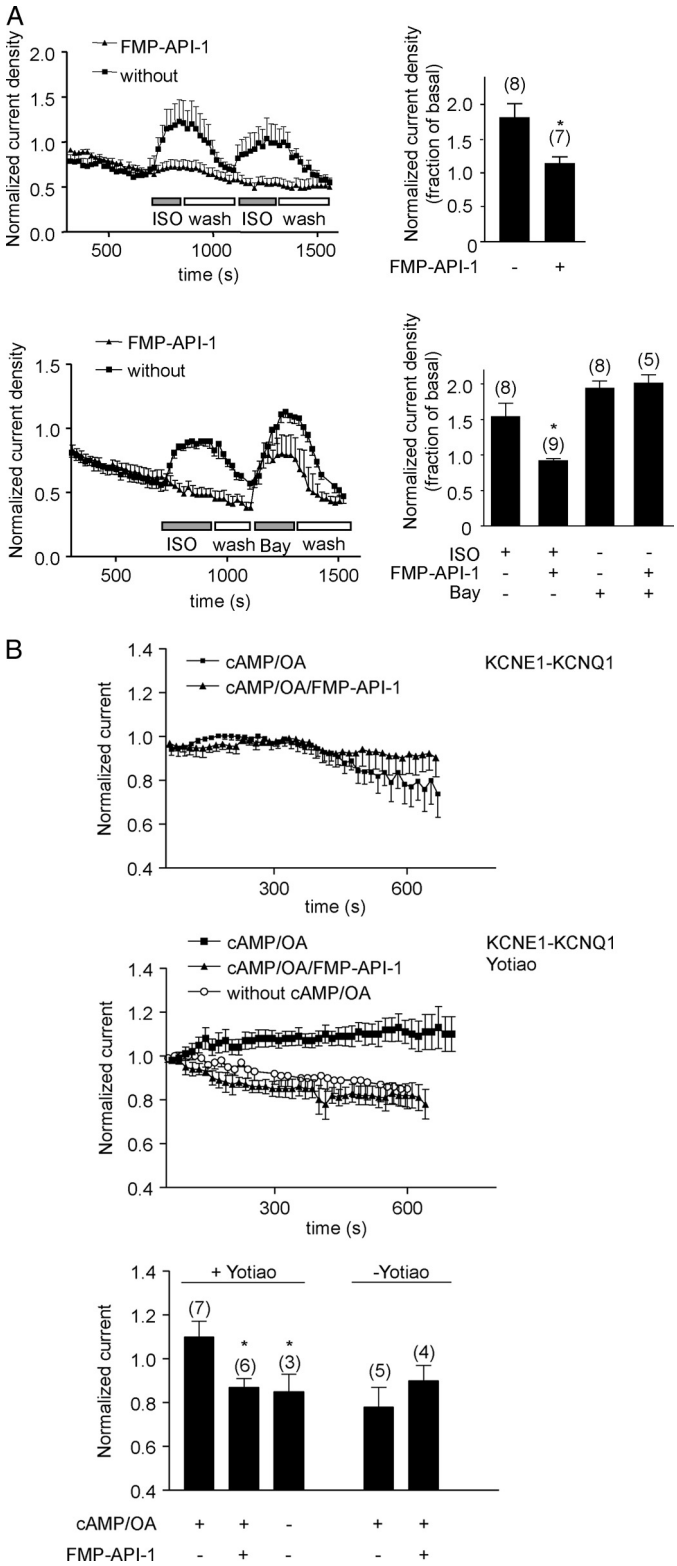

FIGURE 4. **FMP-API-1 inhibits β-adrenoreceptor-induced L-type Ca^{2+}- and I_{Ks} K^+ channel currents.** *A*, L-type Ca^{2+} channel currents in rat neonatal cardiac myocytes were measured using the patch clamp technique. The cells were left untreated (*without*) or perfused with FMP-API-1 (100 μM) via the patch pipette as indicated. Increases in Ca^{2+} currents were induced by ISO (1 μM) (*top*) or the channel activator Bay K8644 (*Bay*; 70 nM) (*bottom*). ISO and Bay were washed out with buffer where indicated (*wash*). Time courses of normalized current densities are shown. *Right*, summaries, means ± S.E.; *, significantly different from untreated cells, $p \leq 0.01$; *n* is indicated by the *numbers* in *parentheses*. *B*, CHO cells transiently expressing either I_{Ks} channels alone (KCNE1-KCNQ1 fusion protein; *top*) or in combination with Yotiao (*middle*) were subjected to a pulse protocol to elicit channel activity. Cells were preincubated with compound and dialyzed with cAMP (200 μM) and okadaic acid (*OA*; 0.2 μM) in the absence or presence of FMP-API-1 (100 μM) via the patch pipette. Time courses of normalized current densities are shown. *Bottom*, summary. Values are mean ± S.E. (*error bars*). *, significantly different from isoproterenol-treated cells, $p \leq 0.01$. *n* is indicated by the *numbers* in *parentheses*.

regulatory subunit KCNE1 were transiently expressed as fusion protein in COS-M7 cells to generate functional channels (26). For activation of PKA, the cells were perfused through the patch pipette with cAMP together with the protein phosphatase inhibitor, okadaic acid. This treatment did not affect K^+ currents (Fig. 4*B*, *top* and *bottom*). However, if the fusion protein and Yotiao were co-expressed, cAMP together with okadaic acid enhanced K^+ currents (Fig. 4*B*, *middle* and *bottom*). The appearance of the current was prevented by challenge of cells with FMP-API-1 (100 μM). The results support the notion that FMP-API-1 prevents Yotiao-dependent tethering of PKA to the channel and thereby the Yotiao-dependent PKA regulation of the channel.

FMP-API-1 Enhances β-Adrenoreceptor-induced cAMP Formation—Prostaglandins E_1 and E_2 (PGE_1 and PGE_2) induce cAMP synthesis through stimulation of EP_2 and EP_4 receptors (33). In HEK293 cells, a multiprotein complex terminates PGE_1-induced cAMP synthesis by establishing a negative feedback loop. The components include among others the AKAP gravin, PKA and cAMP phosphodiesterase-4D3 (PDE4D3; Fig. 5*A*, top) (25). The PGE_1-induced rise in cAMP activates gravin-bound PKA that, in turn, phosphorylates PDE4D3, thereby enhancing its activity and degradation of cAMP in the vicinity of adenylyl cyclases. In addition, AKAP79 targets PKA to adenylyl cyclases V and VI, as shown in both HEK293 cells and mouse brain, thereby facilitating PKA phosphorylation and inhibition of the cyclases (34).

Initially, we tested the impact of FMP-API-1 on the negative feedback regulation of cAMP levels in HEK293 (Fig. 5*A*). The cells were transiently transfected to express CNGC as reporters for near membrane cAMP synthesis and loaded with the Ca^{2+} indicator Fura-2/AM. Stimulation with PGE_1 (1 μM) induces synthesis of cAMP, which binds to CNGC, opening the channels and facilitating Ca^{2+} entry. The rise in Ca^{2+} is reflected by a transient rise in fluorescence signals (Fig. 5*A*, *middle*, *Control*). If degradation of cAMP is prevented with rolipram, a specific inhibitor of PDE4 enzymes (35), or in the presence of the PKA inhibitor H89 or if PKA was uncoupled from AKAPs by the PKA anchoring disruptor peptide Ht31 (10) or with our novel small molecule AKAP-PKA disruptor FMP-API-1 (1 μM), the Ca^{2+} signal (reporting cAMP) persisted (Fig. 5*A*). An inactive control peptide, Ht31-P (10), not binding PKA, did not influence cAMP synthesis. Similar results were obtained if β-adrenoceptors were stimulated with isoproterenol (100 nM; Fig. 5*A*, *bottom*). FMP-API-1 concentration-dependently changed the transient response into a sustained elevation of cAMP. Thus, FMP-API-1 has a similar effect as the well characterized peptide Ht31.

Cardiac myocytes are a major site of expression of adenylyl cyclases V and VI (36) and PDE4 (35, 37). Therefore, we used

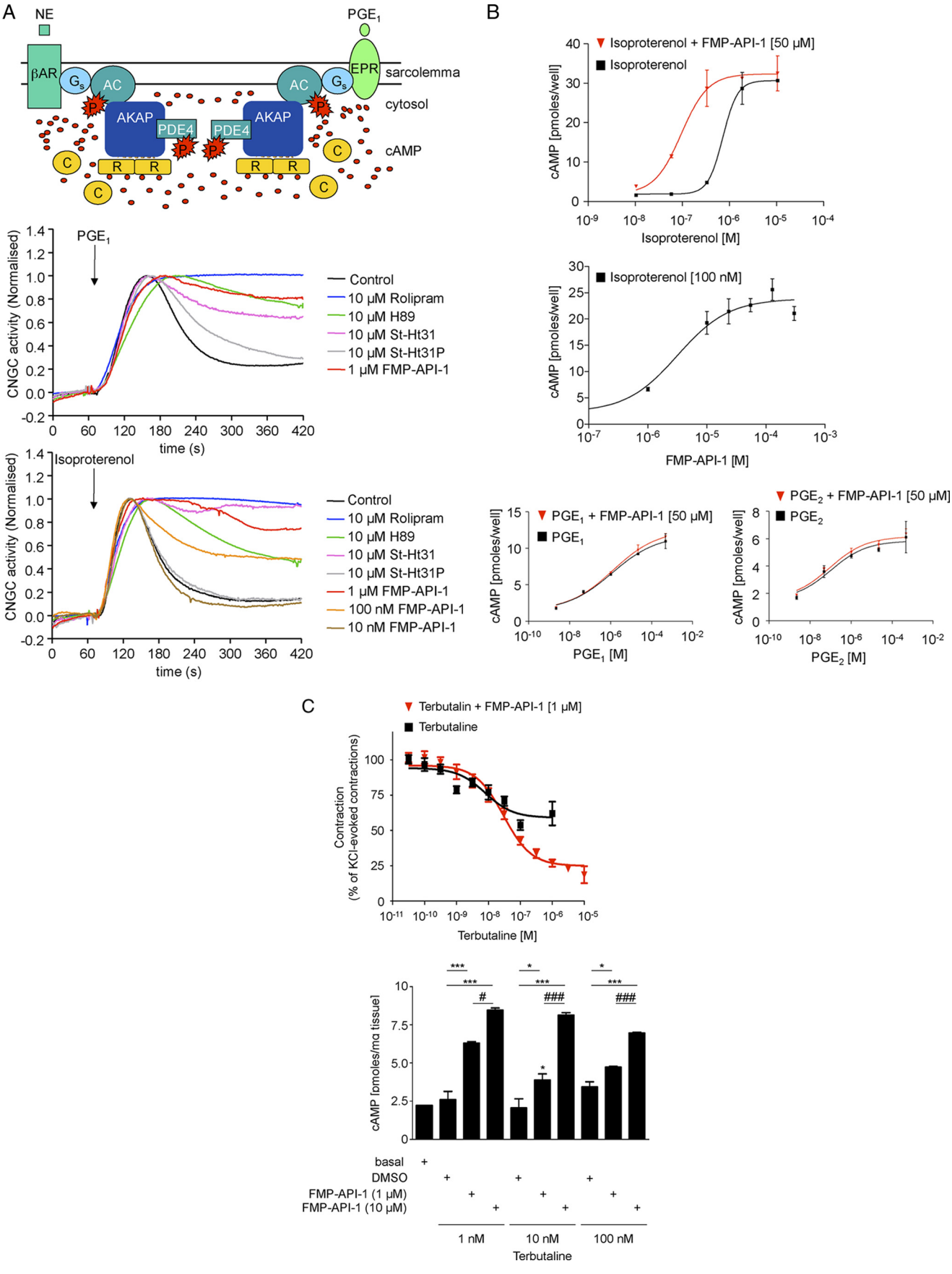

FMP-API-1 to determine whether cAMP synthesis in cardiac myocytes includes a component of negative feedback inhibition controlled by AKAP-PKA interactions. In rat neonatal cardiac myocytes, FMP-API-1 (50 μM) alone did not alter the cAMP level, whereas it augmented isoproterenol-induced cAMP synthesis by 1 order of magnitude, leading to a decrease of the EC_{50} value of isoproterenol from 724 nM (354–1479 nM, 95% confidence interval of the mean) to 95 nM (57–158 nM, 95% confidence interval of the mean) (Fig. 5*B*). FMP-API-1/27 had a similar effect (supplemental Fig. 2*B*). If a constant concentration of isoproterenol (100 nM) was applied and FMP-API-1 was titrated in the concentrations indicated (Fig. 5*B*, *middle*), the EC_{50} for cAMP generation was 3.2 μM (95% confidence interval of the mean). Because FMP-API-1 and FMP-API-1/27 interfere with AKAP-PKA interactions (Figs. 1 and 2), these observations are consistent with the hypothesis that the compounds interfere with a negative feedback regulation of cAMP synthesis in cardiac myocytes that is controlled by AKAP-PKA interactions to limit β-adrenoreceptor-induced cAMP synthesis. The possibility cannot be excluded that the compound interferes with PKA-dependent phosphorylation of PDE4. Interference with the PKA-dependent phosphorylation of PDE4 and thus an increase in its activity (38) in response to β-adrenoreceptor stimulation would contribute to enhancing cAMP synthesis. Thus, the observed rise in cAMP most likely results from both displacement of PKA from the cyclase and inhibition of PDE4 phosphorylation. Therefore, the activation of PKA through FMP-API-1 (Fig. 3) is due to its direct effect on the kinase and to its enhancing effect on the cAMP level.

PGE-dependent signaling in cardiac myocytes leads to increases in cAMP, activating predominantly compartmentalized PKA type I, and does not cause phosphorylations of phospholamban (PLN) and c-TnI (39). Consistently, PGE signaling has not been found to involve either AKAP-PKA- or AKAP-adenylyl cyclase interactions (40, 41). In line with these observations, FMP-API-1 did not enhance either PGE_1- or PGE_2-induced increases of cAMP in neonatal cardiac myocytes (Fig. 5*B*, *bottom*).

It is likely that FMP-API-1 has similar effects on cAMP levels in other cells if they are controlled by AKAP-PKA interactions. In contrast to cardiac myocytes, adenylyl cylcase activation is associated with relaxation in smooth muscle cells. Increases in cAMP levels through β-adrenoreceptor activation promote relaxation of the myometrium via activation of PKA (42). The underlying molecular mechanism involves inhibition of phospholipase C, which is dependent on the plasma membrane-associated interaction of PKA with AKAP150 (43). We investigated the effect of FMP-API-1 on the relaxation of pregnant rat uterus and on cAMP formation. Potassium chloride (KCl) stimulates Ca^{2+} influx in the myometrium by membrane depolarization and evokes contractions. The β_2-adrenoreceptor agonist terbutaline inhibited the KCl-evoked contractions by 41%. In the presence of FMP-AP-1 (1 μM), the maximal contraction-inhibiting effect of terbutaline was increased to 75% ($p < 0.05$; Fig. 5*C*). The terbutaline-induced cAMP accumulations were increased concentration-dependently by 1 and 10 μM FMP-API-1 (Fig. 5*C*). These results indicate that regulation of cAMP synthesis in the myometrium, like that in cardiac myocytes, is controlled by AKAP-PKA interactions terminating β-adrenoreceptor-induced cAMP synthesis. Collectively, these data and our analyses of the effects of FMP-API-1 on PKA-dependent ion channel regulation establish that FMP-API-1 potently interferes with compartmentalized PKA signaling involving AKAP-PKA interactions.

FMP-API-1 Increases PKA-mediated Phosphorylations of Phospholamban and Cardiac Troponin I but Does Not Cause Global Phosphorylation of PKA Substrates or Affect PDEs and Protein Phosphatases—The dual effect of FMP-API-1 on PKA (*i.e.* displacement of PKA from AKAPs and activation of the kinase) suggested that the molecule causes increases in the phosphorylation of PKA substrates in the vicinity of AKAPs, where PKA is concentrated, and generally of substrates in particulate compartments, such as the plasmalemma, because PKA is targeted to such compartments by AKAPs.

Major substrates of PKA in cardiac myocytes are PLN and cardiac troponin I (c-TnI; see Introduction). PLN is anchored to the sarcoplasmic reticulum (SR) and c-TnI is located at the plasmalemma. In response to β-adrenergic stimulation, PKA phosphorylates PLN on serine 16 (44) and c-TnI at serines 23 and 24 (45). The PKA-mediated PLN phosphorylation depends on the interaction of PLN with AKAP18δ (22). Using an antibody that specifically detects the PKA-phosphorylated PLN, an increase in the phosphorylation was observed in response to challenge with FMP-API-1 (100 and 300 μM, 2.6- and 9.3-fold, respectively), isoproterenol (100 nM, 14-fold), or the combination of FMP-API-1 (100 μM) and isoproterenol

FIGURE 5. **In cardiac myocytes, negative feedback regulation of β-adrenoreceptor-induced cAMP synthesis by PKA is based on AKAP-PKA interactions.** *A*, *top*, model of the negative feedback regulation of cAMP synthesis in HEK293 cells (25). Stimulation of EPs with PGE_1 or of β-adrenoceptors (*β-AR*) with adrenergic agonists, such as norepinephrin (*NE*) or isoproterenol, activates the G protein G_s, which in turn stimulates adenylyl cyclase (*AC*). The consequent rise in cAMP activates AKAP-bound PKA. AKAP-associated PKA phosphorylates (*P*) gravin-associated cAMP phosphodiesterase PDE4D, thereby increasing PDE activity and thus inhibiting cAMP accumulation. In HEK293 cells, the AKAP involved is gravin. *Middle*, HEK293 cells, expressing gravin and adenylyl cyclase endogenously, were transiently transfected to express CNGC and loaded with the Ca^{2+} indicator Fura-2. The cells were preincubated with the PDE4 inhibitor rolipram, the PKA inhibitor H89, the PKA-anchoring disruptor peptide Ht31, the inactive control peptide Ht31P, or FMP-API-1 in the indicated concentrations. The peptides were rendered membrane-permeable by coupling to stearate (St-Ht31 and St-Ht31P). At the indicated time point, the cells were stimulated with PGE_1 to induce cAMP synthesis. The rise in cAMP opens CNGC, and Ca^{2+} enters the cells, binds to Fura-2, and thereby generates fluorescence signals, which were imaged. *Bottom*, the same experiment as described above was carried only with isoproterenol (100 nM) as an agonist. Shown are representative results from three independent experiments. *B*, rat neonatal cardiac myocytes were treated with the indicated concentrations of isoproterenol, PGE_1, and PGE_2 in the absence or presence of FMP-API-1 in the indicated concentrations, and cAMP levels were determined by radioimmunoassay. $n = 3$ independent experiments for each experiment. *C*, *top*, contractions of uterine rings isolated from rats on day 22 of pregnancy. The rings were treated with the β_2-adrenoreceptor agonist terbutaline in the indicated concentrations or a combination of terbutaline and FMP-API-1. The responses are expressed as the percentage inhibition of the rhythmic contractions evoked by KCl (mean ± S.E. (*error bars*); $n = 6$ in each group). *Bottom*, cyclic AMP accumulations in rat uterine tissue isolated as indicated above were determined by enzyme immunoassay. The tissue was incubated as indicated (means ± S.E.; $n = 6$ in all groups). Statistically significant differences are indicated as follows: *, $p < 0.05$; ***, $p < 0.001$; #, $p < 0.05$; ###, $p < 0.001$.

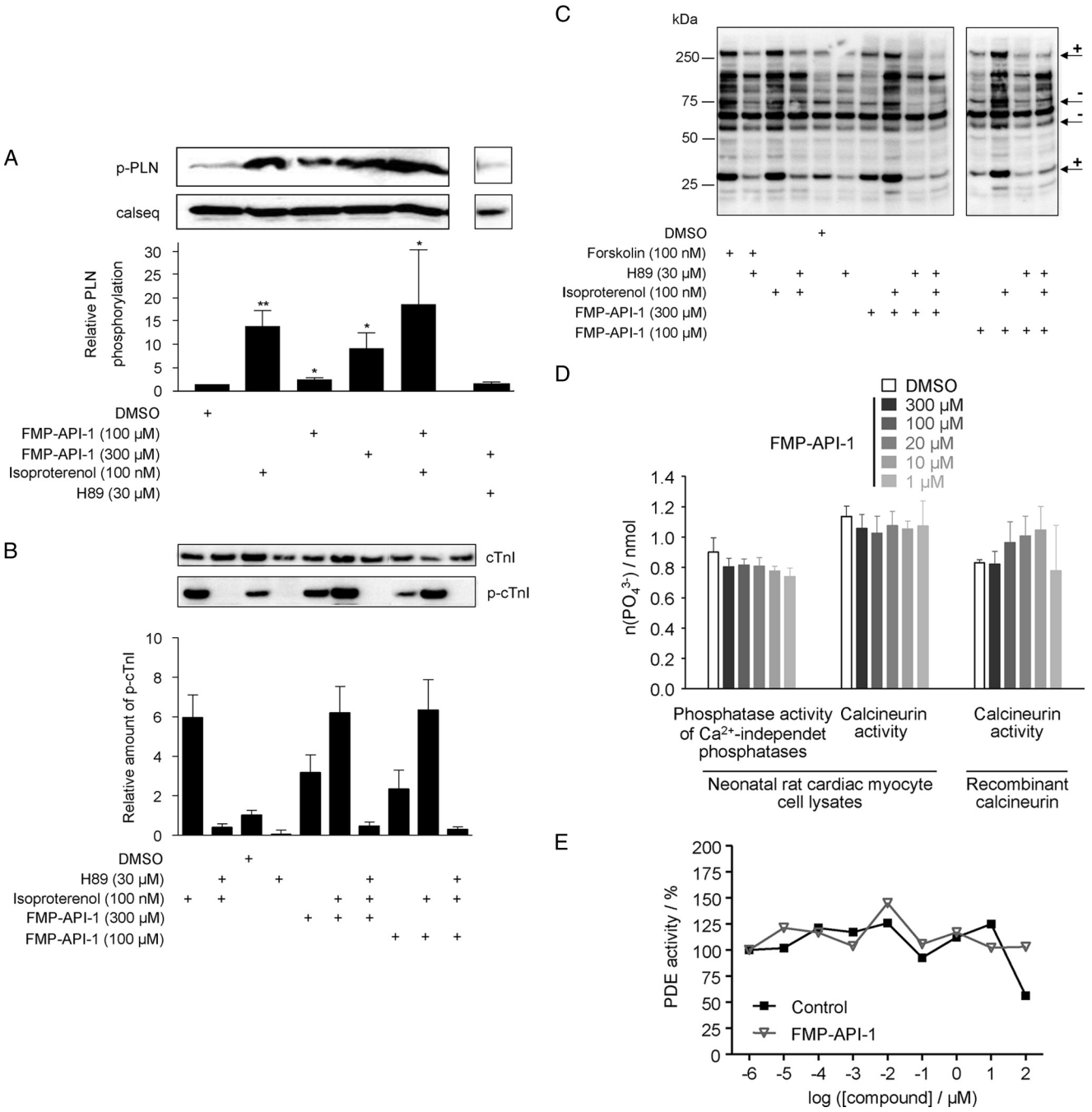

FIGURE 6. **FMP-API-1 enhances PKA-dependent phosphorylation of PLN and c-TnI in cardiac myocytes but does not globally induce phosphorylation of PKA substrates or affect phosphatase or PDE4 activities.** Rat neonatal cardiac myocytes were incubated with the solvent of FMP-API-1, DMSO (0.1%, control), FMP-API-1, isoproterenol, the PKA inhibitor H89, or the indicated combinations of agents. *A*, Western blot analysis with antibodies recognizing PKA-phosphorylated serine 16 of PLN or anti-calsequestrin (loading control). Results are representative of at least five independent experiments for each condition. *Bottom*, semiquantitative analysis of the amounts of phosphorylated PLN. Western blot signals were analyzed densitometrically (means ± S.E. (*error bars*); at least five independent experiments per condition). *, $p < 0.05$; **, $p < 0.005$, statistically significant difference from DMSO-treated control cells. *B*, non-phosphorylated and phosphorylated c-TnI (*c-TnI* and *p-TnI*) were detected by Western blotting. Shown is one representative result from two independent experiments. *Bottom*, semiquantitative analysis of the amounts of phosphorylated c-TnI (mean of two independent experiments). *C*, detection of proteins phosphorylated by PKA at the consensus site RRXS/T. Shown is one representative result from two independent experiments. *Arrows* and *plus signs*, proteins whose PKA phosphorylation increases in response to forskolin, isoproterenol, or FMP-API-1 (100 and 300 μM). H89 reduced these phosphorylation events; *arrows* and *minus signs*, proteins whose PKA phosphorylation increases upon challenge with forskolin and isoproterenol but not upon challenge with FMP-API-1. The forskolin- and isoproterenol-induced phosphorylations were inhibited by H89. *D*, calcineurin and total phosphatase activities were determined. DMSO (0.1%) or FMP-API-1 were added as indicated ($n = 4$, means ± S.E.). *E*, FMP-API-1 does not influence PDE4 activity in cardiac myocytes. Rat neonatal cardiac myocytes were left untreated or incubated with FMP-API-1 in the indicated concentrations. Cell lysates were prepared, and PDE4 activities were measured using 20 μg of protein, 25 μl of cell lysates.

(18-fold; Fig. 6*A*). c-TnI is an AKAP itself (46). The phosphorylation of c-TnI increased in response to FMP-API-1 (100 and 300 μM, 2- and 3-fold, respectively) or to isoproterenol (100 nM, 6-fold; Fig. 6*B*). In combination with isoproterenol, FMP-API-1 did not elevate the phosphorylation level observed in response to isoproterenol alone, presumably be-

cause isoproterenol alone induces saturating phosphorylation of c-TnI. The effect of FMP-API-1 (300 μM) was blocked by the PKA inhibitor H89 (30 μM).

To rule out the possibility that FMP-API-1 induces a global increase in the phosphorylation of PKA substrates, cardiac myocytes were incubated with the molecule, and phosphorylated PKA substrates were detected with an antibody directed against the consensus motif, RR*X*(S/T), phosphorylated by PKA (Fig. 6*C*). Proteins specifically phosphorylated by PKA can be distinguished from proteins not phosphorylated by this kinase because their phosphorylation increases in response to isoproterenol or forskolin and is inhibited by H89. Fig. 6*C* shows two proteins with molecular masses of 250 and 27 kDa (indicated by *arrows* and *plus signs*), whose PKA phosphorylation increases in response to forskolin, isoproterenol, or FMP-API-1 (100 and 300 μM). H89 reduced these phosphorylation events. The phosphorylation of two other proteins, indicated by *arrows* and *minus signs*, increased upon challenge with forskolin and isoproterenol but not upon challenge with FMP-API-1. The forskolin- and isoproterenol-induced phosphorylations were again inhibited by H89. Thus, FMP-API-1 does not globally increase phosphorylation of PKA substrates. Moreover, FMP-API-1 did not inhibit PDE or protein phosphatase activities in lysates from rat neonatal cardiac myocytes, indicating that the increased phosphorylation of proteins by PKA is not due to inhibition of these enzymes (Fig. 6, *D* and *E*). Thus, FMP-API-1-activated PKA most likely phosphorylates a specific subset of target proteins rather than globally the entire pool of possible species. The phosphorylation of a subset of targets is probably catalyzed by specific compartmentalized pools of PKA. Toxic effects of the compounds in the concentrations used were not observed (3-(4,5-dimethylthiazol-2-yl)-2,5-diphenyltetrazolium bromide colorimetric assay; data not shown).

FMP-API-1 Increases Contractility of Cultured Cardiac Myocytes and Isolated Rat Hearts—The observed activation of PKA and increases in PLN and c-TnI phosphorylations by FMP-API-1 led us to investigate whether FMP-API-1 affects the contractility of cardiac myocytes. PKA phosphorylation of PLN increases contraction and of c-TnI enhances relaxation (47, 48). Compared with the solvent DMSO (0.1%) isoproterenol (100 nM) or FMP-API-1 alone (10 μM) increased rates of shortening, of relengthening, and also of absolute cell shortening by 15–20% (Fig. 7*A*). FMP-API-1 consistently inhibited the isoproterenol-induced increases, although the differences did not reach statistical significance. In isolated Langendorff hearts, DMSO also did not have an effect, but FMP-API-1 (10 μM) caused a small but significant increase of 16% in the rate of left ventricular pressure development of 13% in the contraction rate and of 18% in the maximal relaxation rate of the heart (Fig. 7*B*). As expected, isoproterenol increased the three parameters severalfold. The isoproterenol-induced increases of all three parameters were inhibited by around 50% in the presence of FMP-API-1 (10 μM). Thus, the increased level of PKA phosphorylation of PLN in the presence of FMP-API-1 is in line with the observed increase of contraction. The increase in PKA phosphorylation of c-TnI in response to FMP-API-1 is consistent with the observed FMP-API-1-induced enhancement of relaxation. The inhibitory effect of FMP-API-1 on the isoproterenol-induced increases in left ventricular pressure development, contraction rate, and the maximal relaxation rate of the hearts is consistent with the observed inhibitory effect of the small molecule on the isoproterenol-induced increases in L-type Ca^{2+} channel currents (Fig. 4). Taken together, the data indicate that FMP-API-1 leads to both positive inotropic and lusitropic effects by interference with compartmentalized cAMP/PKA signaling.

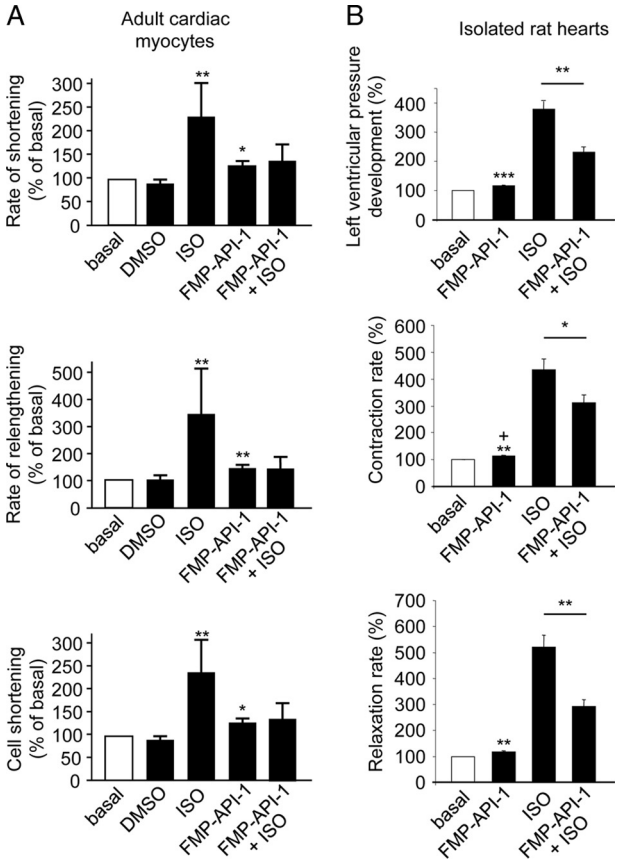

FIGURE 7. **FMP-API-1 increases contractility of cultured adult rat cardiac myocytes and isolated rat hearts.** *A*, adult rat ventricular myocytes were isolated, loaded with Fura-2/AM, and placed under field stimulation. Rates of cell shortening and relengthening and absolute cell shortening were measured under basal conditions (control) and in the presence of the FMP-API-1 solvent DMSO (0.1%), ISO (100 nM), or FMP-API-1 (10 μM; mean ± S.E. (*error bars*), $n \geq 7$ measurements for each condition from at least three different cultures). *B*, left ventricular pressure development, contraction, and relaxation rates were measured in isolated Langendorff rat hearts perfused with vehicle (0.1% DMSO, control), isoproterenol (100 nM), FMP-API-1 (10 μM), or isoproterenol together with FMP-API-1. $n = 6$ hearts were used for each treatment (mean ± S.E.). *, $p < 0.05$ *versus* basal. **, $p < 0.005$; ***, $p < 0.001$ *versus* basal.

DISCUSSION

Based on high throughput screening and subsequent chemical modification, we have identified small molecules, namely FMP-API-1 and its derivative FMP-API-1/27, that disrupt interactions between AKAPs and PKA. The D/D domain at the N terminus of the RII subunits is the interface at which AKAPs interact through their RII-binding domains. Together, NMR, Biacore, and *in vitro* kinase assays show that the molecules reversibly bind to RII subunits C-terminal of the D/D domain (Fig. 1, *F–H*, and supplemental Fig. 1). To date, the

D/D domain has been the only portion of the RII subunits implicated in either direct binding or regulation of binding to AKAPs (5, 9). The fact that the new small molecule disruptors so markedly affect the binding of AKAPs to regulatory subunits without interaction with the core AKAP-regulatory subunit interface and the fact that they act additively with Ht31 peptides (Fig. 1*E*) point to the binding site as a so far unknown allosteric regulatory site. The small molecules interfere with cAMP binding of the regulatory subunits (Figs. 1*H* and 2*B*). It is currently not known whether this occurs through blockade of the cyclic nucleotide-binding domain or binding of the molecule outside the cyclic nucleotide-binding domain, which might lead to a conformational change inhibiting the interaction with cAMP. The region following N-terminally the D/D domain contains an autoinhibitory site (amino acids 92–102 in human RIIα) (49). This inhibitory site binds to the active site cleft of the catalytic subunit in the holoenzyme. The interaction of a small molecule within this region could prevent the inhibitory functioning of this part of the protein, thereby leading to the dissociation, and hence activation, of catalytic subunits. Taken together, not only does the D/D domain seem to interact with RII-binding domains of AKAPs, but additional regions of the regulatory PKA subunits are involved in the interaction.

Interference of the small molecules with the autoinhibitory site may underpin the observed increase in catalytic activity (Fig. 3). In order to fully understand the molecular mechanisms underlying the effects of FMP-API-1 on AKAP-PKA interactions and PKA activity, solved structures of complexes of full-length RII subunits with and without compounds (and of AKAP-R subunit complexes) are needed. However, so far, any attempt to obtain three-dimensional structures of full-length RII subunits has not been successful. In addition, such studies may require compounds binding with higher affinity to RII subunits than those currently available. Our attempts to exactly map the binding region of FMP-API-1 using further truncated versions of RIIα were compromised because the required recombinant proteins were insoluble (*e.g.* RIIα 87–156) or apparently did not fold correctly (*e.g.* RIIα 1–156, indicated by STD NMR experiments; data not shown). We did not consider knockdown of RII subunits as a further approach to confirm that PKA is the FMP-API-1 target because knockdown would lead to a reduction of experimentally detectable RII-AKAP interactions.

With respect to inhibition of AKAP-PKA interactions, FMP-API-1 and derivatives resemble PKA anchoring disruptor peptides, such as Ht31 and AKAP18δ-derived peptides, which block AKAP-PKA interactions by binding to the D/D domain of regulatory subunits (6, 10, 12, 50). Several experiments show that FMP-API-1 and the peptides have similar effects on cellular functions. For example, both agents ablate β-adrenoreceptor-induced increases in L-type Ca^{2+} and I_{KS} channel currents and inhibit negative feedback regulation of adenylyl cyclase-dependent cAMP synthesis (Figs. 4 and 5) (12, 25, 32, 51). Thus, blocking of the canonical AKAP-interacting site, namely the D/D domain, either directly with peptides or indirectly through the binding of a small molecule to an allosteric site, inhibits AKAP-RII subunit interactions. Although the efficacy for inhibition of AKAP-RII interactions with the small molecules identified is considerably lower than that with the peptides (IC_{50} values are μM *versus* nM), a major advantage of small molecules compared with peptides is their wider applicability for cell and animal experiments. Efficient transfer of peptides to disrupt the interactions in cells and living animals requires costly efforts, including viral transfection or generation of cell-penetrating peptides (12, 50, 52, 53). Thus, the small molecules discovered here pave the way to new approaches for elucidating functions of AKAP-PKA interactions *in vivo*.

In cardiac myocytes, FMP-API-1 enhances β-adrenoreceptor-induced increases in cAMP levels (Fig. 5) and thus reveals a novel mechanism terminating β-adrenoreceptor-dependent signaling in the heart. AKAP79/150 tethers PKA to adenylyl cyclases V and VI to phosphorylate it, rapidly terminating cAMP synthesis upon activation of PKA in the brain and in HEK293 cells (34, 54). Because adenylyl cyclases V and VI are highly relevant cyclases in cardiac myocytes (55), and FMP-API-1 disrupts the AKAP150-PKA interaction in these cells (Fig. 2), it is conceivable that the compound blunts negative feedback regulation of these cyclases by interference with this interaction. However, other AKAPs may link PKA to adenylyl cyclases in cardiac myocytes. For example, mAKAPβ is associated with adenylyl cyclase V (54), and targeting of PKA by Yotiao to various other adenylyl cyclases has recently been observed in neurons (56). Further evidence confirming that FMP-API-1 interferes with AKAP-PKA interactions that control adenylyl cyclase activities stems from the experiments in uterine tissue (Fig. 5*C*). The molecule enhances β-adrenoreceptor-induced cAMP production in uterus preparations, presumably by interference with AKAP150-PKA interactions, which play a role in controlling uterine contraction (57). Thus, attenuation of adenylyl cyclase activity in response to β-adrenergic agonists regularly seems to rely on AKAP-PKA interactions. Our analyses of the effects of FMP-API-1 on prostaglandin E-stimulated adenylyl cyclase activity in cardiac myocytes shows no FMP-API-1-dependent increase in cAMP formation in response to either PGE_1 or PGE_2. The cognate eicosanoid E prostaglandin receptors (EPs) couple to the G_s/adenylyl cyclase system (33), and EP signaling mainly involves compartmentalized PKA type I (39). AKAP-PKA interactions have not been found to be involved in EP signaling (40, 41). This is consistent with our observations that FMP-API-1 has no effect on EP signaling. The negative feedback regulation may involve PKA phosphorylation of PDE4. Inhibition of AKAP-PKA interactions may reduce such phosphorylation and thereby prevent enhanced cAMP degradation, which in turn would contribute to elevation of the cAMP level in the presence of the inhibitor.

The classical function of AKAPs is to concentrate PKA at defined cellular sites. FMP-API-1 displaces PKA from AKAP18δ (Fig. 2), which tethers PKA to PLN (22), but this does not result in lower levels of PLN phosphorylation. In contrast, PKA-dependent phosphorylation of PLN in cardiac myocytes is increased by FMP-API-1 challenge (Fig. 6). This unexpected observation might be explained by the dual effect of FMP-API-1. The FMP-API-1-induced direct activation of

PKA leads to a local rise in the activity of PKA in the vicinity of PLN where PKA is concentrated by AKAP18δ (22). Activated PKA, in turn, phosphorylates this substrate. This seems feasible when disruption (*i.e.* displacement of PKA from AKAP18δ) and activation occur simultaneously. In addition, the FMP-API-1-induced direct activation of PKA at the AKAP18δ-PKA complex is probably enhanced through the FMP-API-1-induced increases in cAMP levels in the presence of adrenergic stimuli. The same reasons are likely to account for the FMP-API-1-induced and PKA-dependent increases in the phosphorylation of c-TnI, which is an AKAP itself (46). The increased PLN and c-TnI phosphorylation would account for the resulting positive inotropic and lusitropic effects on cultured adult cardiac myocytes and isolated hearts (Fig. 7). Bond and co-workers (13) and Patel *et al.* (50) had shown that uncoupling of PKA from AKAPs with the PKA anchoring disruptor peptides Ht31 and AKAD in both cultured cardiac myocytes and intact hearts decreases phosphorylation of PLN and c-TnI (52, 53). The decrease is most likely due to the lack of PKA-activating capabilities of the peptides (23). Bond and co-workers (13, 53) observed a positive inotropic effect in response to uncoupling PKA from AKAPs. Thus, either disruption of AKAP-PKA interactions alone or disruption of the interactions in conjunction with PKA activation results in a positive inotropic response. This outcome is potentially highly relevant therapeutically because the development of small molecule disruptors of AKAP-PKA interactions, either with or without the ability to activate PKA, could pave the way for a novel treatment of chronic heart failure. The classical approaches to elicit positive inotropic responses rely on stimulation of β-adrenoceptors, inhibition of cAMP synthesis by blockade of PDE3, or inhibition of Ca^{2+} channels with heart glycosides. All of these approaches constitute initially effective treatments, but chronic treatments based on these concepts harm the failing heart and may even increase mortality, as in the case of PDE3 inhibitors (by 28%) (58). One reason for the failure of the approaches that elevate cellular cAMP levels (β-agonists and PDE blockers) may be that PKA is constitutively and globally activated throughout the cells (59). Local interference with defined cellular signaling processes using AKAP-PKA disruptors may lead to a more effective treatment with fewer side effects because PKA may not randomly phosphorylate its substrates (Fig. 6). Generally, the specificity and diversity of protein-protein interactions permits potentially highly selective pharmacological interference with defined cellular processes and thus disruption of specific protein-protein interactions promises better drugs (6).

Several observations underline that the effects of FMP-API-1 and FMP-API-1/27 on cardiac myocytes and intact hearts are not due to off target effects, although the chemical structure of FMP-API-1 may suggest that it has the potential to react with other proteins. (i) The identification of inactive FMP-API-1 derivatives, such as FMP-API-1/26 (Fig. 1*B*), indicates that the molecule does not nonspecifically bind to proteins. (ii) FMP-API-1 interferes with β-adrenergic but not with $PGE_{1/2}$ signaling (see above). (iii) FMP-API-1 did not prevent direct activation of L-type Ca^{2+} channels (Fig. 4*A*). (iv) FMP-API-1 did not cause random increases of PKA-dependent substrate phosphorylations (Fig. 6). (v) Activities of several kinases (apart from PKA) that are involved in cardiac myocyte control (including ErbB1, MEK1, ERK1 and -2, ROCK1 and -2, PKCα, CaMKIIα, and GSK3β) are affected by FMP-API-1 only to a minor extent (supplemental Fig. 3). Consistently, antibodies directed against substrate proteins phosphorylated by PKC, CaMKII, or Akt did not detect changes in the phosphorylation pattern of proteins in cardiac myocytes treated with FMP-API-1 for 30 min (100 or 300 μM; data not shown). (vi) FMP-API-1 did not influence protein phosphatase and phosphodiesterase activities (Figs. 6, *D* and *E*). Thus, the molecule apparently interferes selectively with compartmentalized cAMP signaling.

In summary, the identification of the small molecules described here lays the groundwork for the development of high affinity small molecules disrupting the interaction of PKA with AKAPs as well as for revealing novel mechanisms underlying this interaction. Such molecules provide an invaluable tool for new approaches to study functions of AKAP-PKA interactions in living cells and animals. Moreover, they have the potential to be developed as highly targeted therapeutics for the treatment of diseases that are associated with altered cAMP signaling but that are not addressed sufficiently by conventional pharmacotherapy, such as chronic heart failure.

Acknowledgments—We thank Andrea Geelhaar, Beate Eisermann, Anita Neumann, Jenny Eichhorst, and Matthias Pipow for excellent technical assistance. We are grateful to Peter Schlegel for supporting Langendorff heart experiments and Dr. Giuseppe Cacciatore for help with SPR measurements.

REFERENCES

1. Taylor, S. S., Kim, C., Cheng, C. Y., Brown, S. H., Wu, J., and Kannan, N. (2008) *Biochim. Biophys. Acta* **1784,** 16–26
2. Newlon, M. G., Roy, M., Morikis, D., Hausken, Z. E., Coghlan, V., Scott, J. D., and Jennings, P. A. (1999) *Nat. Struct. Biol.* **6,** 222–227
3. Kinderman, F. S., Kim, C., von Daake, S., Ma, Y., Pham, B. Q., Spraggon, G., Xuong, N. H., Jennings, P. A., and Taylor, S. S. (2006) *Mol. Cell* **24,** 397–408
4. Gold, M. G., Lygren, B., Dokurno, P., Hoshi, N., McConnachie, G., Taskén, K., Carlson, C. R., Scott, J. D., and Barford, D. (2006) *Mol. Cell* **24,** 383–395
5. Sarma, G. N., Kinderman, F. S., Kim, C., von Daake, S., Chen, L., Wang, B. C., and Taylor, S. S. (2010) *Structure* **18,** 155–166
6. Hundsrucker, C., and Klussmann, E. (2008) *Handb. Exp. Pharmacol.* **186,** 483–503
7. McCahill, A. C., Huston, E., Li, X., and Houslay, M. D. (2008) *Handb. Exp. Pharmacol.* **186,** 125–166
8. Carnegie, G. K., Means, C. K., and Scott, J. D. (2009) *IUBMB Life* **61,** 394–406
9. Skroblin, P., Grossmann, S., Schäfer, G., Rosenthal, W., and Klussmann, E. (2010) *Int. Rev. Cell Mol. Biol.* **283,** 235–330
10. Carr, D. W., Hausken, Z. E., Fraser, I. D., Stofko-Hahn, R. E., and Scott, J. D. (1992) *J. Biol. Chem.* **267,** 13376–13382
11. Alto, N. M., Soderling, S. H., Hoshi, N., Langeberg, L. K., Fayos, R., Jennings, P. A., and Scott, J. D. (2003) *Proc. Natl. Acad. Sci. U.S.A.* **100,** 4445–4450
12. Hundsrucker, C., Krause, G., Beyermann, M., Prinz, A., Zimmermann, B., Diekmann, O., Lorenz, D., Stefan, E., Nedvetsky, P., Dathe, M., Christian, F., McSorley, T., Krause, E., McConnachie, G., Herberg, F. W., Scott, J. D., Rosenthal, W., and Klussmann, E. (2006) *Biochem. J.* **396,** 297–306

13. Mauban, J. R., O'Donnell, M., Warrier, S., Manni, S., and Bond, M. (2009) *Physiology* **24,** 78–87
14. Wells, J. A., and McClendon, C. L. (2007) *Nature* **450,** 1001–1009
15. Yin, H., and Hamilton, A. D. (2005) *Angew Chem. Int. Ed. Engl.* **44,** 4130–4163
16. Buchwald, P. (2010) *IUBMB Life* **62,** 724–731
17. Henn, V., Edemir, B., Stefan, E., Wiesner, B., Lorenz, D., Theilig, F., Schmitt, R., Vossebein, L., Tamma, G., Beyermann, M., Krause, E., Herberg, F. W., Valenti, G., Bachmann, S., Rosenthal, W., and Klussmann, E. (2004) *J. Biol. Chem.* **279,** 26654–26665
18. Hundsrucker, C., Skroblin, P., Christian, F., Zenn, H. M., Popara, V., Joshi, M., Eichhorst, J., Wiesner, B., Herberg, F. W., Reif, B., Rosenthal, W., and Klussmann, E. (2010) *J. Biol. Chem.* **285,** 5507–5521
19. Herberg, F. W., Maleszka, A., Eide, T., Vossebein, L., and Tasken, K. (2000) *J. Mol. Biol.* **298,** 329–339
20. Meyer, B., Klein, J., Mayer, M., Meinecke, R., Moller, H., Neffe, A., Schuster, O., Wulfken, J., Ding, Y., Knaie, O., Labbe, J., Palcic, M. M., Hindsgaul, O., Wagner, B., and Ernst, B. (2004) *Ernst Schering Res. Found. Workshop* **44,** 149–167
21. Alvarez, J., Hamplova, J., Hohaus, A., Morano, I., Haase, H., and Vassort, G. (2004) *J. Biol. Chem.* **279,** 12456–12461
22. Lygren, B., Carlson, C. R., Santamaria, K., Lissandron, V., McSorley, T., Litzenberg, J., Lorenz, D., Wiesner, B., Rosenthal, W., Zaccolo, M., Taskén, K., and Klussmann, E. (2007) *EMBO Rep.* **8,** 1061–1067
23. Klussmann, E., Maric, K., Wiesner, B., Beyermann, M., and Rosenthal, W. (1999) *J. Biol. Chem.* **274,** 4934–4938
24. Stefan, E., Wiesner, B., Baillie, G. S., Mollajew, R., Henn, V., Lorenz, D., Furkert, J., Santamaria, K., Nedvetsky, P., Hundsrucker, C., Beyermann, M., Krause, E., Pohl, P., Gall, I., MacIntyre, A. N., Bachmann, S., Houslay, M. D., Rosenthal, W., and Klussmann, E. (2007) *J. Am. Soc. Nephrol.* **18,** 199–212
25. Willoughby, D., Wong, W., Schaack, J., Scott, J. D., and Cooper, D. M. (2006) *EMBO J.* **25,** 2051–2061
26. Terrenoire, C., Houslay, M. D., Baillie, G. S., and Kass, R. S. (2009) *J. Biol. Chem.* **284,** 9140–9146
27. Wang, W. (1999) *Am. J. Physiol.* **277,** F826–F831
28. Abdelaziz, A. I., Segaric, J., Bartsch, H., Petzhold, D., Schlegel, W. P., Kott, M., Seefeldt, I., Klose, J., Bader, M., Haase, H., and Morano, I. (2004) *J. Mol. Med.* **82,** 265–274
29. Lipinski, C. A., Lombardo, F., Dominy, B. W., and Feeney, P. J. (2001) *Adv. Drug Deliv. Rev.* **46,** 3–26
30. Huang, L. J., Durick, K., Weiner, J. A., Chun, J., and Taylor, S. S. (1997) *J. Biol. Chem.* **272,** 8057–8064
31. Hulme, J. T., Westenbroek, R. E., Scheuer, T., and Catterall, W. A. (2006) *Proc. Natl. Acad. Sci. U.S.A.* **103,** 16574–16579
32. Chen, L., Kurokawa, J., and Kass, R. S. (2005) *J. Biol. Chem.* **280,** 31347–31352
33. Sugimoto, Y., and Narumiya, S. (2007) *J. Biol. Chem.* **282,** 11613–11617
34. Bauman, A. L., Soughayer, J., Nguyen, B. T., Willoughby, D., Carnegie, G. K., Wong, W., Hoshi, N., Langeberg, L. K., Cooper, D. M., Dessauer, C. W., and Scott, J. D. (2006) *Mol. Cell* **23,** 925–931
35. Houslay, M. D., Baillie, G. S., and Maurice, D. H. (2007) *Circ. Res.* **100,** 950–966
36. Willoughby, D., and Cooper, D. M. (2007) *Physiol. Rev.* **87,** 965–1010
37. Lynch, M. J., Baillie, G. S., Mohamed, A., Li, X., Maisonneuve, C., Klussmann, E., van Heeke, G., and Houslay, M. D. (2005) *J. Biol. Chem.* **280,** 33178–33189
38. Sette, C., and Conti, M. (1996) *J. Biol. Chem.* **271,** 16526–16534
39. Di Benedetto, G., Zoccarato, A., Lissandron, V., Terrin, A., Li, X., Houslay, M. D., Baillie, G. S., and Zaccolo, M. (2008) *Circ. Res.* **103,** 836–844
40. Hayes, J. S., Brunton, L. L., and Mayer, S. E. (1980) *J. Biol. Chem.* **255,** 5113–5119
41. Zaccolo, M. (2006) *Eur. J. Cell Biol.* **85,** 693–697
42. Sanborn, B. M., Yue, C., Wang, W., and Dodge, K. L. (1998) *Rev. Reprod.* **3,** 196–205
43. Dodge, K. L., Carr, D. W., Yue, C., and Sanborn, B. M. (1999) *Mol. Endocrinol.* **13,** 1977–1987
44. Chu, G., Lester, J. W., Young, K. B., Luo, W., Zhai, J., and Kranias, E. G. (2000) *J. Biol. Chem.* **275,** 38938–38943
45. Dong, W. J., Jayasundar, J. J., An, J., Xing, J., and Cheung, H. C. (2007) *Biochemistry* **46,** 9752–9761
46. Sumandea, C. A., Garcia-Cazarin, M. L., Bozio, C. H., Sievert, G. A., Balke, C. W., and Sumandea, M. P. (2011) *J. Biol. Chem.* **286,** 530–541
47. El-Armouche, A., and Eschenhagen, T. (2009) *Heart Fail. Rev.* **14,** 225–241
48. Solaro, R. J., Rosevear, P., and Kobayashi, T. (2008) *Biochem. Biophys. Res. Commun.* **369,** 82–87
49. Taylor, S. S., Buechler, J. A., and Yonemoto, W. (1990) *Annu. Rev. Biochem.* **59,** 971–1005
50. Patel, H. H., Hamuro, L. L., Chun, B. J., Kawaraguchi, Y., Quick, A., Rebolledo, B., Pennypacker, J., Thurston, J., Rodriguez-Pinto, N., Self, C., Olson, G., Insel, P. A., Giles, W. R., Taylor, S. S., and Roth, D. M. (2010) *J. Biol. Chem.* **285,** 27632–27640
51. Hulme, J. T., Lin, T. W., Westenbroek, R. E., Scheuer, T., and Catterall, W. A. (2003) *Proc. Natl. Acad. Sci. U.S.A.* **100,** 13093–13098
52. Fink, M. A., Zakhary, D. R., Mackey, J. A., Desnoyer, R. W., Apperson-Hansen, C., Damron, D. S., and Bond, M. (2001) *Circ. Res.* **88,** 291–297
53. McConnell, B. K., Popovic, Z., Mal, N., Lee, K., Bautista, J., Forudi, F., Schwartzman, R., Jin, J. P., Penn, M., and Bond, M. (2009) *J. Biol. Chem.* **284,** 1583–1592
54. Dessauer, C. W. (2009) *Mol. Pharmacol.* **76,** 935–941
55. Pierre, S., Eschenhagen, T., Geisslinger, G., and Scholich, K. (2009) *Nat. Rev. Drug Discov.* **8,** 321–335
56. Piggott, L. A., Bauman, A. L., Scott, J. D., and Dessauer, C. W. (2008) *Proc. Natl. Acad. Sci. U.S.A.* **105,** 13835–13840
57. Dodge, K. L., Carr, D. W., and Sanborn, B. M. (1999) *Endocrinology* **140,** 5165–5170
58. Packer, M., Carver, J. R., Rodeheffer, R. J., Ivanhoe, R. J., DiBianco, R., Zeldis, S. M., Hendrix, G. H., Bommer, W. J., Elkayam, U., Kukin, M. L., *et al.* (1991) *N. Engl. J. Med.* **325,** 1468–1475
59. Antos, C. L., Frey, N., Marx, S. O., Reiken, S., Gaburjakova, M., Richardson, J. A., Marks, A. R., and Olson, E. N. (2001) *Circ. Res.* **89,** 997–1004

Small Molecule AKAP-Protein Kinase A (PKA) Interaction Disruptors That Activate PKA Interfere with Compartmentalized cAMP Signaling in Cardiac Myocytes

Frank Christian, Márta Szaszák, Sabine Friedl, Stephan Drewianka, Dorothea Lorenz, Andrey Goncalves, Jens Furkert, Carolyn Vargas, Peter Schmieder, Frank Götz, Kerstin Zühlke, Marie Moutty, Hendrikje Göttert, Mangesh Joshi, Bernd Reif, Hannelore Haase, Ingo Morano, Solveig Grossmann, Anna Klukovits, Judit Verli, Róbert Gáspár, Claudia Noack, Martin Bergmann, Robert Kass, Kornelia Hampel, Dmitry Kashin, Hans-Gottfried Genieser, Friedrich W. Herberg, Debbie Willoughby, Dermot M. F. Cooper, George S. Baillie, Miles D. Houslay, Jens Peter von Kries, Bastian Zimmermann, Walter Rosenthal and Enno Klussmann

J. Biol. Chem. 2011, 286:9079-9096.
doi: 10.1074/jbc.M110.160614 originally published online December 22, 2010